

NASA/CR—1998-202328



# Small Engine Technology (Set) Task 8 Aeroelastic Prediction Methods

## Final Report

Chris D. Eick and Jong-Shang Liu  
AlliedSignal Engines, Phoenix, Arizona

Prepared under Contract NAS3-27483

National Aeronautics and  
Space Administration

Lewis Research Center

---

June 1998

## Acknowledgments

AlliedSignal Engines would like to thank our technical monitor at the NASA LeRC Structural Dynamics Branch, Mr. David Janetzke, for his assistance with the programmatic issues in this effort. For the UNSFLO evaluation, we are grateful for the assistance of Dr. Reza Abhari of Ohio State University. The FREPS evaluation would not have been possible without the extensive assistance of Dr. Durbha Murthy (formerly of NASA LeRC and now with AK). In addition, Dr. Dan Hoyniak of Westinghouse provided substantial assistance during our evaluations of the SFLOW code and his advice was greatly appreciated. For the TURBO-AK evaluation, Dr.'s Milind Bakhle and Rakesh Srivastava of NASA LeRC provided outstanding support and encouragement which enabled AE to successfully complete our evaluation. We also thank Dr. Dennis Huff (NASA LeRC) who provided advice and assistance with the FREPS and TURBO-AK evaluations. Finally, we thank Mr. George Stefko (NASA LeRC) for his many suggestions, both technical and programmatic, on this effort.

This report was prepared as an account of work sponsored by an agency of the United States Government. Neither the United States Government nor any agency thereof, nor any of their employees, makes any warranty, express or implied, or assumes any legal liability or responsibility for the accuracy, completeness, or usefulness of any information, apparatus, product, or process disclosed, or represents that its use would not infringe privately owned rights. Reference herein to any specified commercial product, process, or service by trade name, trademark, manufacturer, or otherwise, does not necessarily constitute or imply its endorsement, recommendation, or favoring by the United States Government or any agency thereof. The views and opinions of authors expressed herein do not necessarily state or reflect those of the United States Government or any agency thereof.

Trade names or manufacturers' names are used in this report for identification only. This usage does not constitute an official endorsement, either expressed or implied, by the National Aeronautics and Space Administration.

Available from

NASA Center for Aerospace Information  
7121 Standard Drive  
Hanover, MD 21076  
Price Code: A04

National Technical Information Service  
5287 Port Royal Road  
Springfield, VA 22100  
Price Code: A04

## FOREWORD

AlliedSignal Engines would like to thank our technical monitor at the NASA LeRC Structural Dynamics Branch, Mr. David Janetzke, for his assistance with the programmatic issues in this effort. For the UNSFLO evaluation, we are grateful for the assistance of Dr. Reza Abhari of Ohio State University. The FREPS evaluation would not have been possible without the extensive assistance of Dr. Durbha Murthy (formerly of NASA LeRC and now with AE). In addition, Dr. Dan Hoyniak of Westinghouse provided substantial assistance during our evaluations of the SFLOW code and his advice was greatly appreciated. For the TURBO-AE evaluation, Dr. 's Milind Bakhle and Rakesh Srivastava of NASA LeRC provided outstanding support and encouragement which enabled AE to successfully complete our evaluation. We also thank Dr. Dennis Huff (NASA LeRC) who provided advice and assistance with the FREPS and TURBO-AE evaluations. Finally, we thank Mr. George Stefko (NASA LeRC) for his many suggestions, both technical and programmatic, on this effort.

**This page intentionally left blank.**

## TABLE OF CONTENTS

	<u>Page</u>
LIST OF ACRONYMS AND ABBREVIATIONS	vi
SUMMARY	vii
1.0 INTRODUCTION	1
2.0 BACKGROUND	2
3.0 AEROELASTIC METHODOLOGY DEVELOPMENT	4
3.1 Development of Execution Procedures for UNSFLO and FREPS	7
4.0 AEROELASTIC CODE EVALUATIONS	10
4.1 Test Case Formulation	10
4.2 UNSFLO Evaluation	13
4.2.1 General	13
4.2.2 Code Description	13
4.2.3 Flutter Evaluation	14
4.2.3.1 Analysis Methodology	14
4.2.3.2 Inviscid/Coupled Viscous Solution Results	16
4.2.3.3 Unsteady Flow Comparisons	20
4.2.3.4 Aerodynamic Damping Computation	25
4.2.4 Synchronous Vibrations	27
4.2.5 AE Suggestions for Further Development of the UNSFLO Code	27
4.3 Freps Evaluation	31
4.3.1 General	31
4.3.2 Code Description	31
4.3.3 Results	32
4.3.4 Further Explanation of SFLOW Problem Areas	33
4.3.5 AE Suggestions for SFLOW/FREPS Code Improvements	33
4.4 Turbo-AE Evaluation	39
4.4.1 General	39
4.4.2 Code Description	39
4.4.3 NASA E <sup>3</sup> Fan Test Case	40
4.4.4 Flutter Vibrations on F2 Test Case	41
4.4.5 Steady Results	41
4.4.6 Unsteady Results	44
4.4.7 Go-Forward Plan For Turbo-AE	47
5.0 SUMMARY	48
6.0 REFERENCES	49

## LIST OF FIGURES

<u>Fig. No.</u>	<u>Title</u>	<u>Page</u>
1	Progression of Fan Designs Moves from Inserted-Dampered Designs to Damperless Blisk Rotors	2
2	Demonstrated Fan Technologies Were Combined in the Successful TFE731-60 Fan	3
3	AE Aeroelastic Methodology Development Program Plan	4
4	AE SET/AST Code Evaluation Procedure Using “Steady” Test Data	5
5	GUIde Consortium Aeroelastic Measurement Program Using AE TFE731-2 HP Turbine at Ohio State University	6
6	Proposed AE Fan Blisk Aeroelastic Measurement Program at Ohio State University	6
7	Aeroelastic Analysis Methodology Process (Aero)	7
8	Results From Hot to On-Point 2-D Geometry Conversion for Case S1	8
9	Aeroelastic Methodology Analysis Flowchart (Mechanical)	9
10	Fan Blisk Aeroelastic Test Cases	10
11	Normalized Vibrational Mode Shape for Case F2	12
12	Analysis Methodology Flowchart	14
13	UNSFLO Computational Grid	15
14	UNSFLO Steady Flow Vectors for Typical Test Cases	17
15	UNSFLO Steady Results for Case F1	18
16	UNSFLO Steady Results for Case NF2	19
17	UNSFLO Unsteady Surface Pressures (Max, Min, Average) for Case F1	21
18	UNSFLO Unsteady Surface Pressures (Max, Min, Average) for Case NF2	22
19	UNSFLO Unsteady Pressure Contours for Various Times In the Blade Vibrational Cycle (IBPA=0°)	23
20	UNSFLO Unsteady Pressure Contours for Various Times In the Blade Vibrational Cycle (IBPA=32.7°)	24
21	UNSFLO Variation of Damping with IBPA for Case F2	26
22	UNSFLO Synchronous Unsteady Pressure Contours for Synchronous Vibration Case S3	29
23	Typical SFLOW Computational H-Grid	35
24	SFLOW Solution has a Leading Edge Mach Number Overspeed for All Test Cases	36
25	SFLOW Flow Vectors Show Overspeed at Leading Edge	37
26	3-D Euler Code (DENTON) Results for Typical FREPS Case	38
27	Comparison of NASA and AlliedSignal Unsteady Results for the E <sup>3</sup> Fan	41
28	Computational Grid For TURBO-AE Analyses	42
29	Steady Flow TURBO-AE/DAWES Comparison for Case F2 at Mid-Span	43
30	Steady Flow TURBO-AE/DAWES Comparison for Case F2 at 95 Percent Span	44
31	Test Case F2 TURBO-AE Work/Cycle Results for Various Inter Blade Phase Angles	47

## LIST OF TABLES

<u>Table No.</u>	<u>Title</u>	<u>Page</u>
1	UNSFLO AERODYNAMIC DAMPING COMPUTATION FOR AE FAN FLUTTER CASES	26
2	FREPS COMPLETION STATUS	32
3	TURBO-AE UNSTEADY RESULTS FOR CASE F2 WITH IBPA = 0° AND 180°	46
4	TURBO-AE UNSTEADY RESULTS FOR CASE F2 WITH IBPA = 32.7°	46

## LIST OF ACRONYMS AND ABBREVIATIONS

<b><u>Abbreviation</u></b>	<b><u>Definition</u></b>
AE	AlliedSignal Engines, Phoenix, AZ
AST	Advanced Subsonic Technology
AZ	Arizona
CFD	Computational Fluid Dynamics
DAWES	AlliedSignal 3-D Viscous Steady Flow CFD Solver
EO	Engine Order
FREPS	NASA Developed Forced Response Prediction System Aeroelastic Computer Code
GUIde	Government/University/Industry Consortium for Research on Bladed Disks
IBPA	Inter Blade Phase Angle
IR&D	Independent Research and Development
LeRC	Lewis Research Center
NASA	National Aeronautics and Space Administration
SET	Small Engine Technology
SFLOW	Steady Flow Solver Computer Program
TFE731	AE Turbofan Engine
TURBO-AE	NASA/Mississippi State University Developed 3-D Aeroelastic Computer Code
UNSFLO	MIT Developed/AE Modified, Quasi 3-D Aeroelastic Computer Code
2-D	Two-Dimensional
3-D	Three-Dimensional



## SUMMARY

AlliedSignal Engines, in cooperation with NASA LeRC, completed an evaluation of recently developed aeroelastic computer codes using test cases from the AlliedSignal Engines fan blisk database. Test data for this task includes strain gage, light probe, performance, and steady-state pressure information obtained for conditions where synchronous or flutter vibratory conditions were found to occur. Aeroelastic codes evaluated include the quasi 3-D UNSFLO (developed at MIT and modified to include blade motion by AlliedSignal), the 2-D FREPS (developed by NASA LeRC), and the 3-D TURBO-AE (under development at NASA LeRC). Six test cases each where flutter and synchronous vibrations were found to occur were used for evaluation of UNSFLO and FREPS. In addition, one of the flutter cases was evaluated using TURBO-AE. The UNSFLO flutter evaluations were completed for 75 percent radial span and provided good agreement with the experimental test data. Synchronous evaluations were completed for UNSFLO but further enhancement needs to be added to the code before the unsteady pressures can be used to predict forced response vibratory stresses. The FREPS evaluations were hindered as the steady flow solver (SFLOW) was unable to converge to a solution for the transonic flow conditions in the fan blisk. This situation resulted in all FREPS test cases being attempted but no results were obtained during the present program. Currently, AlliedSignal is evaluating integrating FREPS with our existing steady flow solvers to bypass the SFLOW difficulties. The TURBO-AE steady flow solution provided an excellent match with the AlliedSignal Engines calibrated DAWES 3-D viscous solver. Finally, the TURBO-AE unsteady analyses also matched experimental observations by predicting flutter for the single test case evaluated.



**NAS3-27483**  
**NASA SMALL ENGINE TECHNOLOGY (SET) TASK 8**  
**AEROELASTIC PREDICTION METHODS**  
**FINAL REPORT**

## **1.0 INTRODUCTION**

The primary objective of the Aeroelastic Prediction Methods program is to develop a Computational Fluid Dynamics (CFD) based aeroelastic analysis methodology for use at AlliedSignal Engines (AE). This CFD based aeroelastic technology will provide critical enhancement to the currently used empirical methods that have been applied successfully at AE in the design of numerous gas turbine engines but have recently been shown to be inadequate for advanced rotor designs such as fan blisks.

Specific CFD based aeroelastic codes evaluated in this effort include:

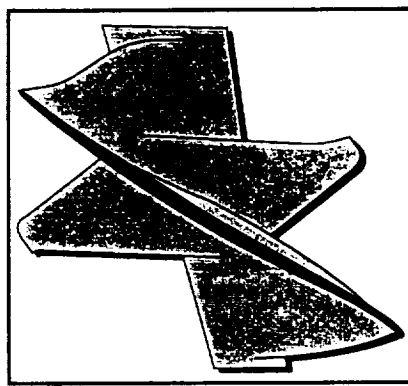
- UNSFLO (MIT developed, AE modified), quasi 3-D, viscous unsteady aerodynamic code which allows for blade motion
- FREPS (NASA developed), 2-D strips, potential steady/unsteady solver, integrated with structural analysis codes
- TURBO-AE (NASA development in process), 3-D viscous, integrated with structural analysis codes

Test cases for the code evaluations will come from the AE fan blisk database which includes two rotors having different aerodynamic designs that were fabricated and tested at AE facilities. Flutter vibrations were observed during the testing of these rotors even though empirical correlations suggested that the designs should be “flutter free”. In addition, synchronous vibrations exceeded acceptable levels and were substantially higher than inserted blade rotor designs with identical aerodynamic geometry’s.

These experimental results clearly outline the need for technology improvements in the area of flutter and synchronous response prediction capabilities and provide strong justification for the continuing leadership provided by NASA in this arena.

## 2.0 BACKGROUND

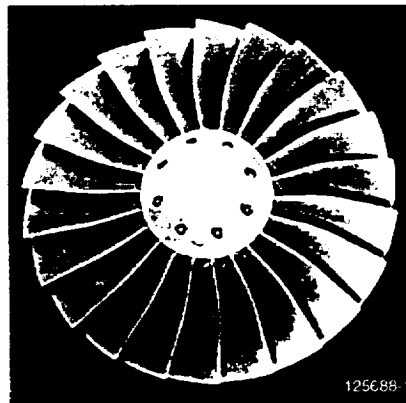
Since the early 1970s, AE has had extensive experience in design, development, and production of turbofan engines for commercial and military applications. Most of these applications have been in the medium bypass ratio range (BPR = 3 to 5), requiring single-stage transonic axial fans utilizing mid-span dampers (see Figure 1(a) for fan picture). AE's aeroelastic design approach for these engines has been to apply empirically based design guidelines to prevent flutter and minimize synchronous (forced) vibrations. This procedure, in conjunction with the stabilizing feature of the mid-span dampers has proven successful in controlling both flutter and synchronous blade vibrations thus eliminating the need for more detailed CFD type analyses.



**a) Inserted Blade Fan**

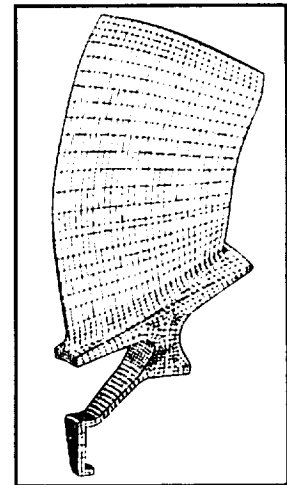
- High Aspect Ratio
- Mid Span Dampers

G7999-17A



**b) TFE731-60 Inserted Blade Fan**

- Low Aspect Ratio
- Damperless
- Improved Performance



**c) Blisk Fan**

- Low Aspect Ratio
- Damperless
- Reduced Weight

**Figure 1. Progression of Fan Designs Moves from Inserted-Dampened Designs to Damperless Blisk Rotors**

The 5000-pound-thrust-class TFE731-60 engine is the latest addition to the AE turbofan product line. It received FAA certification on May 1, 1995, and has entered production for the Falcon 900EX aircraft. Aerodynamic and mechanical technologies and features incorporated in the TFE731-60 fan component are summarized in Figure 2. Key among the features contributing to the very high level of aerodynamic performance of the -60 is the damperless, low-aspect-ratio, fan with moderately swept rotor blades (see Figure 1(b) and Figure 2). Demonstrated -60 design point (typical climb/cruise condition) fan aerodynamic performance parameters are also noted in Figure 2. The -60 fan's polytropic efficiency (over 90 percent) is state of the art, especially for the relatively small size class of the -60 fan. Again, in the area of aeroelasticity

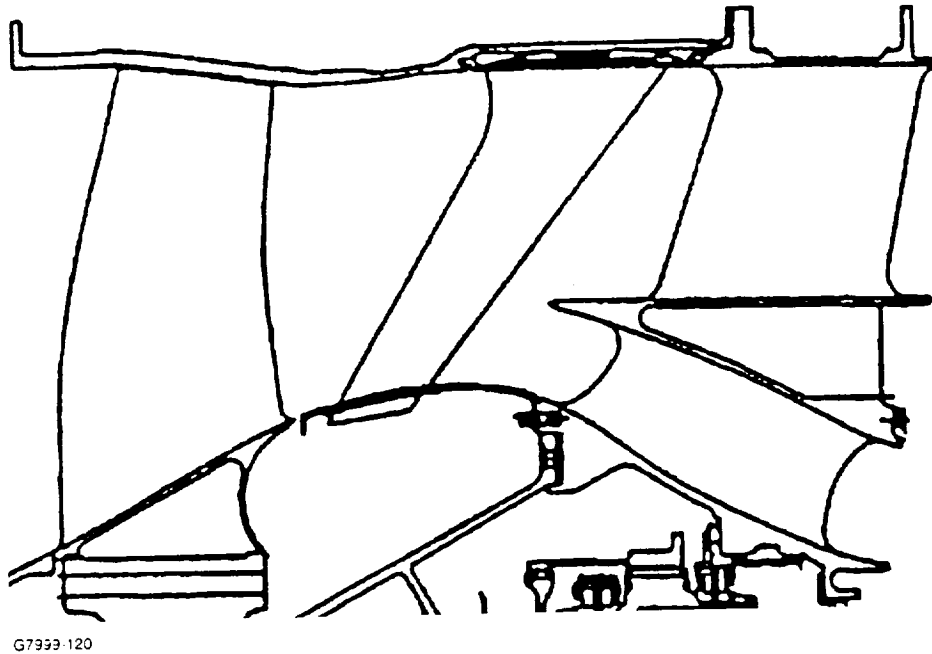


**Figure 2. TFE731-60 Fan Cross Section.**

the existing empirical guidelines provided sufficient capability to design the fan to be flutter free and have low levels of synchronous vibrations even though the -60 rotor was free of mid-span dampers.

Following the -60, the next step in AE technology development is to make a fan rotor in a blisk version (integrally bladed rotor) which affords significantly reduced weight for the fan module. Two blisk versions with slightly different aerodynamic geometry were manufactured (see Figure 1(c) for a cross section) in a subscale rig size and tested in the AE fan rig facility. Results from this testing has shown that the previously acceptable empirical aeroelastic guidelines do not provide sufficient margin to prevent flutter or control synchronous vibrations when the rotor is designed in a blisk configuration having no external damping mechanisms.

A key technology required to achieve our goal of designing damperless blisk fan rotors will be the introduction of CFD type aeroelastic analyses into our design process. AE is working in close coordination with NASA Lewis Research Center to develop this analytical capability. This report summarizes the first step in this process through the contract NAS3-27483 Small Engine Technology (SET) Task 8. A follow-on effort to continue these activities will be completed under the NASA Advanced Subsonic Technology (AST) program. In addition, AE provides internal support through IR&D and various engine development programs to enhance aeroelastic capabilities.

### 3.0 AEROELASTIC METHODOLOGY DEVELOPMENT

As previously mentioned, prior to beginning this task, AE aeroelastic analyses were based primarily on empirical methods and CFD type computations were not completed. This situation is shown in the left side of Figure 3 which outlines the program plan to improve aeroelastic methodology at AE. During the 1996-1998 time frame AE will conduct code validation activities under the NASA SET and AST programs. Codes included in this effort include those previously mentioned plus recently developed GUIde consortium tools. A critical future activity will be to further validate these aeroelastic tools using unsteady pressure measurements from rotors executing flutter and synchronous vibrations. The final goal for all these efforts will be to have a fully calibrated aeroelastic design system in place for year 2000 engines.

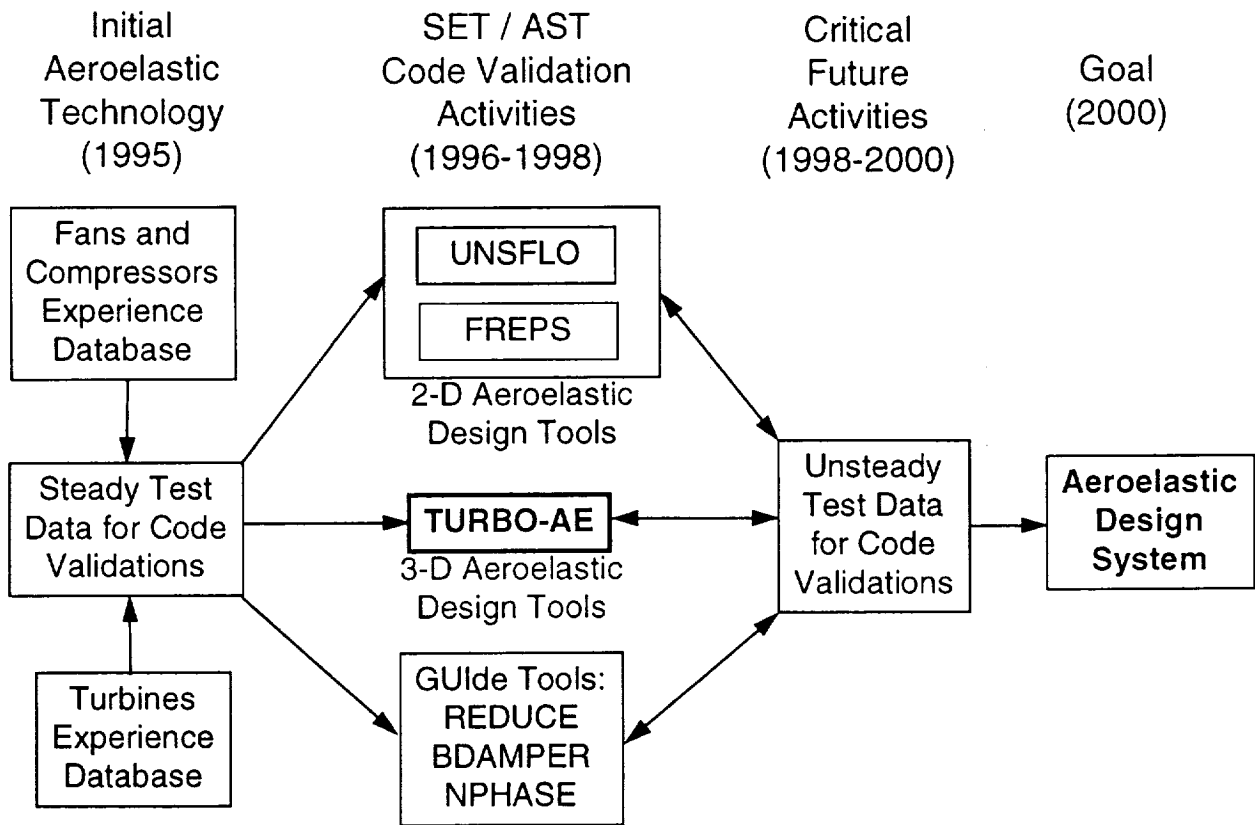


**Figure 3. AE Aeroelastic Methodology Development Program Plan.**

The overall SET and AST aeroelastic methodology development programs will concentrate on both Fan and Turbine code evaluations. This process includes using "Steady" test data which simply consists of operating the codes at conditions (flow, speed, pressure ratio, etc.) where flutter or synchronous vibrations were observed in engine or rig testing. A flowchart of this process is given in Figure 4. The basic process is simply to execute the codes and see if the predicted results are consistent with the measured data from the engine or rig. If the match is good, the code will be directly integrated into the AE design system. When the match is poor, further analysis will

be completed to quantify deficiencies and the results will be reported to the code developer for future improvements.

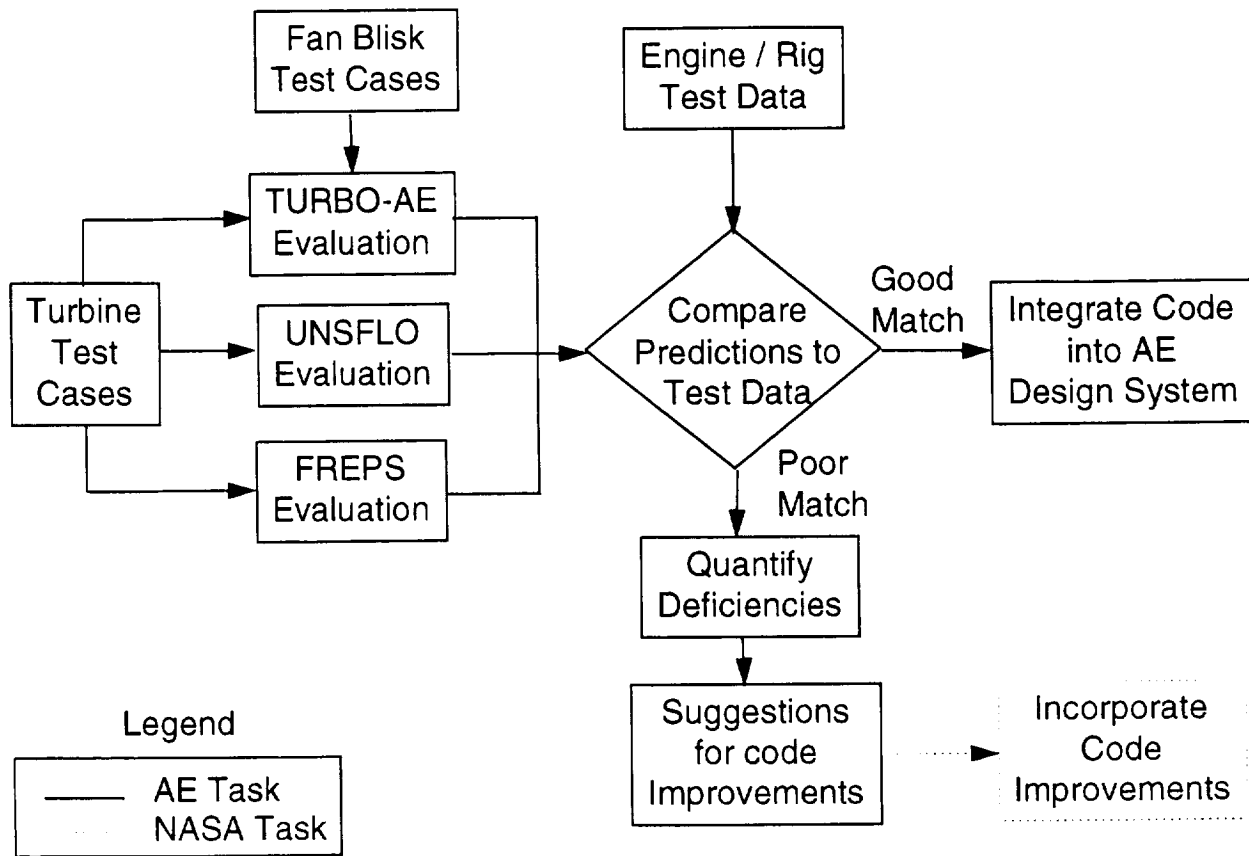


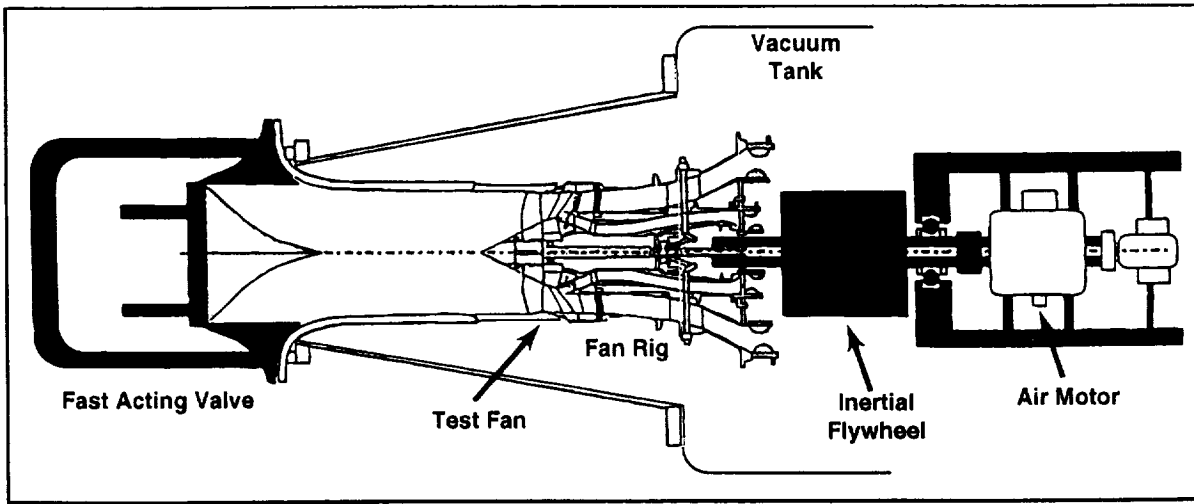
Figure 4. AE SET/AST Code Evaluation Procedure Using “Steady” Test Data.

Although validation codes with “Steady” test data is the obvious first step, AE feels strongly that eventual calibration with “unsteady” data including blade surface pressures, light probe measurements, and strain gage data will be required. Two such programs are described in Figures 5 and 6. The GUIde Consortium program (Figure 5) uses an AE TFE731-2 HP turbine instrumented with Kulite unsteady pressure transducers and strain gages to obtain unsteady synchronous vibration data. Another critical program, currently unfunded, is the proposed AE fan blisk aeroelastic measurement effort (Figure 6) which will provide unsteady pressure measurements for a rotor in a flutter condition. The test setup in Figure 6 is shown in the Ohio State Short Duration facility but might also be run in a longer duration facility.



- 41 Upstream Vanes / 78 Rotor Blades
- Subsonic Flow Conditions
- 4% Field Failure Rate (HCF) prior to redesign
  - Forced Response vibrations at vane passing frequency
  - 5th Mode (2nd torsion)
  - 20 kHz
- Redesigned rotor eliminated vibration problems

**Figure 5. GUIde Consortium Aeroelastic Measurement Program Using an AE TFE731-2 HP Turbine at Ohio State University.**



**Ohio State University Short Duration Test Facility**

- Provides high-response unsteady pressure and strain data at a reasonably low cost
- Ideal for calibration of unsteady CFD codes

G7999-18

**Figure 6. Proposed AE Fan Blisk Aeroelastic Measurement Program at Ohio State University.**



### 3.1 Development of Execution Procedures for UNSFLO and FREPS

Since AE had not completed any CFD type aeroelastic analyses prior to this program, development of appropriate preprocessors comprised a substantial portion of the SET Task 8 effort. The goal for these preprocessors is to provide a seamless integration with the AE aerodynamic and mechanical design systems. Ease of use is critical in these activities so designers who do not regularly run aeroelastic analyses can easily utilize the tools developed to determine the aeroelastic issues pertinent to their rotor configuration.

The process flowchart for integrating Aeroelastic analyses with the AE Aerodynamic design system is shown in Figure 7. Typically the designer will have either an aero "Bankfile" or 3-D steady CFD results from the AE DAWES code available prior to running an aeroelastic analysis. This information will basically consist of blade and flowpath geometry along with flow conditions (pressures, temperatures, velocities, etc.).

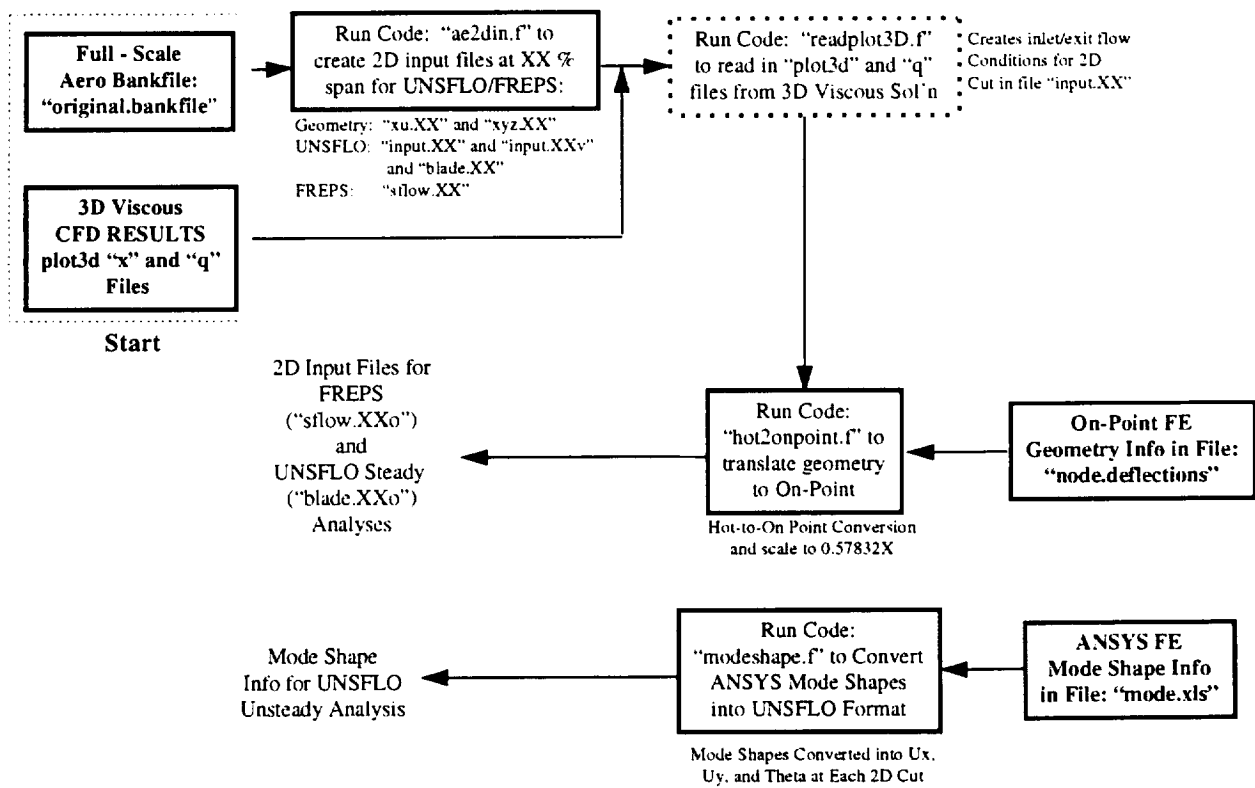
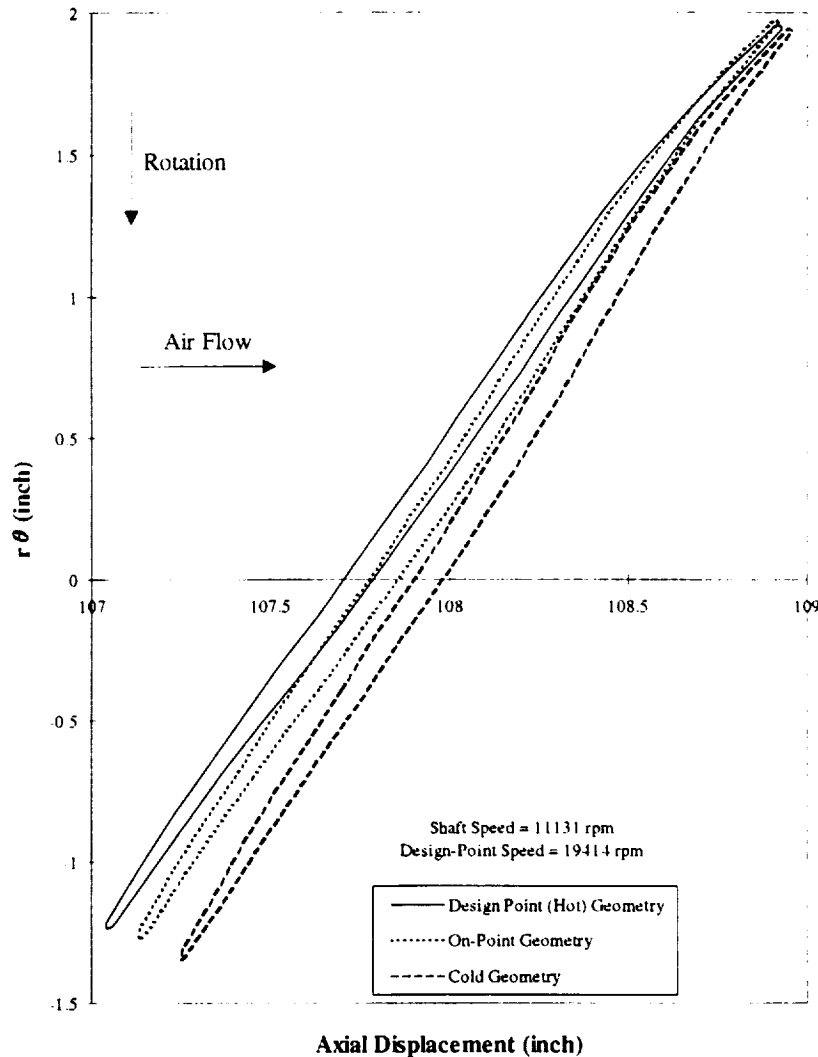


Figure 7. Aeroelastic Analysis Methodology Process (Aero).

A pre-processor "ae2din" was developed for UNSFLO and FREPS. This code, reads the Bankfile and cuts the three-dimensional geometry into two-dimensional strips following either the streamline or the grid line at any user specified spanwise location. The user has the choice to dump either a UNSFLO or FREPS input file. For UNSFLO simulation, "ae2din" will create a 2D geometry file along with the input file which contains the flow information, such as inlet angle, pressure ratio, and Reynolds number. It also creates the stream tube height information based on the 2D axisymmetric solution in the "bankfile" or the "plot3d" file from any 3D solutions. For FREPS simulation, "ae2din" will create one file including the geometry and the flow information.

Following completion of the “ae2din” procedure, the next step in the process is to perform a hot-to-on-point translation which moves the 2-D strip geometry from the “hot” shape used by the aero designers to an “on-point” shape appropriate for aeroelastic analyses at part speed conditions. The code “hot2onpoint” was created for this process and uses the input file “node.deflections” which is generated from structural finite element analysis. A typical result from this process is shown in Figure 8 which shows the difference between the “hot” and “on-point” geometry for a typical test case.



**Figure 8. Results From Hot to On-Point 2-D Geometry Conversion for Case S1.**

The interface of aeroelastic analyses with the AE Mechanical design process is outlined in Figure 9. This process again starts with the Bankfile and uses the pre-existing code MESHI to generate a structural finite element mesh. The macro “subscale.mac” is then executed to generate a subscale rotor size if required. Next, the user runs pre-existing macros to convert the structural finite element geometry from the “hot” aero shape in the bankfile to

“on-point” used in the aeroelastic analyses. The user then runs pre-existing vibratory stress macros to develop the mode shapes for the aeroelastic analyses.

The development of these pre-processors to interface with existing AE aerodynamic and mechanical design systems consumed a substantial amount of effort in the SET Task 8 program. This effort will pay back several fold as now the aeroelastic analysis process is reasonably well defined and further improvements will be easy to incorporate.

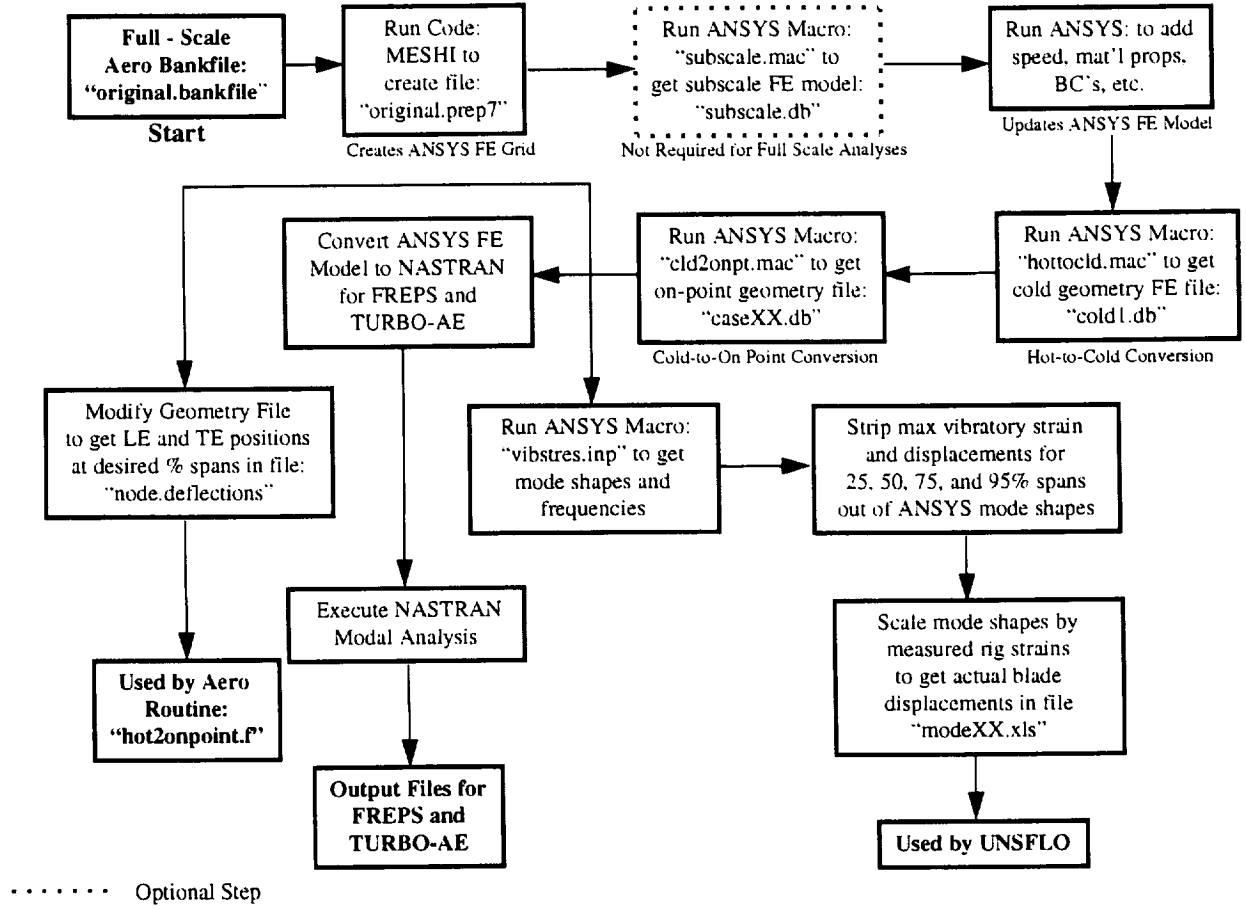


Figure 9. Aeroelastic Methodology Analysis Flowchart (Mechanical).

#### 4.0 AEROELASTIC CODE EVALUATIONS

AE attempted/completed code evaluations for numerous flutter and synchronous vibration cases using the UNSFLO and FREPS codes. In addition, one flutter case was completed using the TURBO-AE code. Test case preparation consumed a significant portion of the code evaluation process and is described in the following section. Additional sections are included for the UNSFLO, FREPS, and TURBO-AE evaluations.

##### 4.1 Test Case Formulation

Fourteen fan blisk test cases have been selected for the UNSFLO and FREPS flutter and synchronous vibration evaluations. Each flutter test case, labeled F1 to F6 on the fan map in Figure 10, was chosen to coincide with operating conditions where flutter vibrations were found to occur. The flutter cases all occurred with clean inlet operating conditions on the test rig, i.e. no distortion screens were required to initiate or sustain the flutter. Two additional cases, labeled NF1 and NF2, were developed to test the codes at conditions where flutter was not observed during testing. These cases correspond to the design point for each fan rotor. The synchronous cases, labeled S1-S6 in Figure 10, were chosen to coincide with conditions where high synchronous vibrations were measured during the rotor testing.

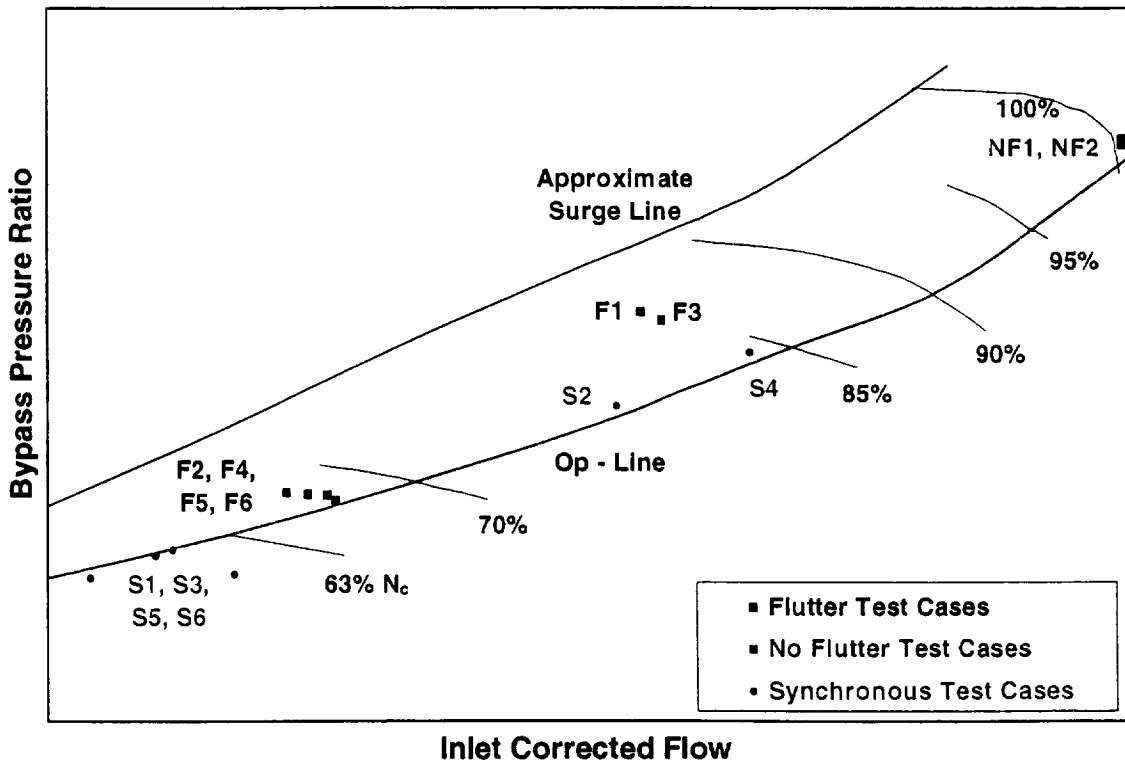
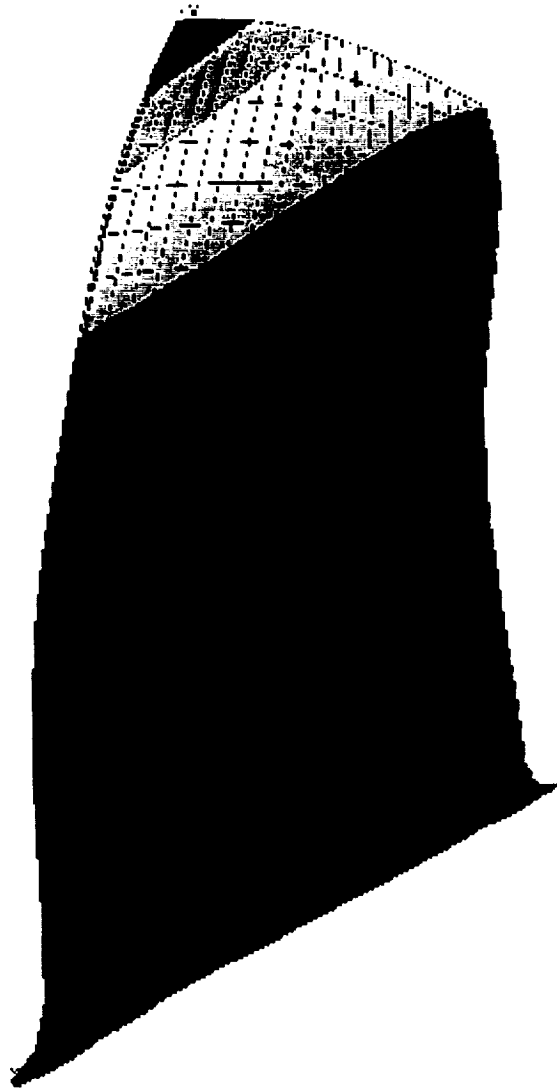


Figure 10. Fan Blisk Aeroelastic Test Cases.

The flutter cases, F1 - F6, are divided into two zones: low speed (F2, F4, F5, F6) and high speed (F1, F3) . The synchronous cases, S1 - S6, consisted of Mode 1 (first flexural) and Mode 2 (second flexural) crossings.

Although the pre-processor "ae2din" is used to create input files for the UNSFLO and FREPS analyses, there is still a need to update critical parameters if a more accurate analysis is required. The primary reason for this step is that the Bankfile uses flow information from an axisymmetric inviscid flow solver. More accurate information is obtained from using the DAWES 3-D viscous flow solver. Updated parameters from these analyses were used for the present code evaluation. This additional level of analysis is required during the code validation stage and may not be required during typical design analyses in the future.

Spectrum analysis of strain gage signals indicated that the flutter vibration frequency corresponds to the first flexural mode of the airfoil for all the test cases F1 - F6. Detailed structural finite element analyses from the code ANSYS ®<sup>1</sup>, a registered trademark of SAS IP, revealed that the airfoil leading edge displacement is approximately twice that observed at the trailing edge indicating that the first flexural mode has a significant torsional component. This situation can be seen from Figure 11 which shows the vibrational mode shape for test case F2 computed for a fixed-root airfoil. It should be noted that the mode shape displacements shown in Figure 11 represent the vector sum of the three (x, y, z) vibrational components.



**Figure 11. Normalized Vibrational Mode Shape for Case F2.**

## **4.2 UNSFLO Evaluation**

### **4.2.1 General**

UNSFLO evaluations were completed for cases F1-F6, S1-S6, and NF1-NF2. The best results were obtained for the flutter/no-flutter cases as the code has developed post processors available to analyze the predictions. The synchronous cases were run using the UNSFLO code but further post-processing was not completed as this would require integration with a structural finite element code.

It is important to note that all UNSFLO analyses were completed for the 75 percent span only. This choice was made to allow comparison of results against AE empirical databases which typically use the 75 percent span location.

### **4.2.2 Code Description**

The computer code UNSFLO is a quasi 3-D Reynolds-averaged, unsteady multi-blade row Navier Stokes solver developed by Giles<sup>2</sup>. Specific details on the theory and formulation of the UNSFLO code can be seen in the references so only an overview will be presented here<sup>2,3,4</sup>.

UNSFLO couples an inviscid solution of the Euler equations in the outer region to a Navier-Stokes solution in the O-layer wrapped around the airfoil. Quasi 3-D effects are included through the addition of streamtube height in the third dimension although this feature of the code was not used for the current analyses. The inviscid grid used in these analyses is a structured H type mesh while the viscous computations use an O-grid wrapped around the airfoil. A Baldwin-Lomax algebraic turbulence model is used in the viscous part of the solution.

A modification to include blade motion in UNSFLO was incorporated by Abhari and Giles<sup>5</sup>. In this formulation the 2-D airfoil section is allowed harmonic motion in the x, y, and  $\alpha$  directions (where  $\alpha$  represents the torsional component of the mode shape). All grid motion is confined to the inner O-grid where the viscous Navier-Stokes flow equations are solved. The outer region H-grid remains unchanged during the airfoil motion. UNSFLO has the capability to model conditions with various interblade phase angles.

Since the airfoil motion is confined to the O-grid which is fairly small, the vibrational displacements input to UNSFLO were scaled down from the actual values measured on the fan rig. Typical motions were on the order of 0.0001 inch for the UNSFLO analyses. This limitation is not thought to be serious, as the real concern of the engine designer is to determine the flutter-free stability limits of the airfoil and not the actual flutter vibrational amplitude.

### 4.2.3 Flutter Evaluation

The code evaluation process used in this task was to exercise UNSFLO at several test cases where flutter was found to occur and see if the code predictions match experimental observations. This determination is made from the computation of the aerodynamic work per cycle by UNSFLO. A positive work per cycle indicates that the airfoil extracts energy from the airstream during each vibrational cycle. If this extracted energy exceeds that dissipated by the material structural damping, then flutter can be expected to occur.

#### 4.2.3.1 Analysis Methodology

An overall flowchart of the UNSFLO analysis procedure is shown in Figure 12. Following the hot-to-on point geometry conversion previously discussed, the next step in the analysis procedure is to complete the steady inviscid Euler solution. This step can be completed quickly (typically less than 30 minutes of computational time) and full solution convergence is not required. The next step is to develop the steady coupled inviscid/viscous solution. This effort is substantially more computationally intensive and takes an overnight run to converge to a solution.

After the steady solutions have converged to acceptable levels the unsteady flutter analyses can begin. The user inputs the vibrational mode shape and period along with the desired interblade phase angle. UNSFLO then determines the unsteady solution. As with the steady coupled solution, this effort is computationally demanding and typically required from 10 to 30 hours of CPU time to converge on an advanced workstation. After completion of the UNSFLO unsteady computations, a simple post-processing effort is undertaken to determine the aerodynamic work per vibrational cycle.

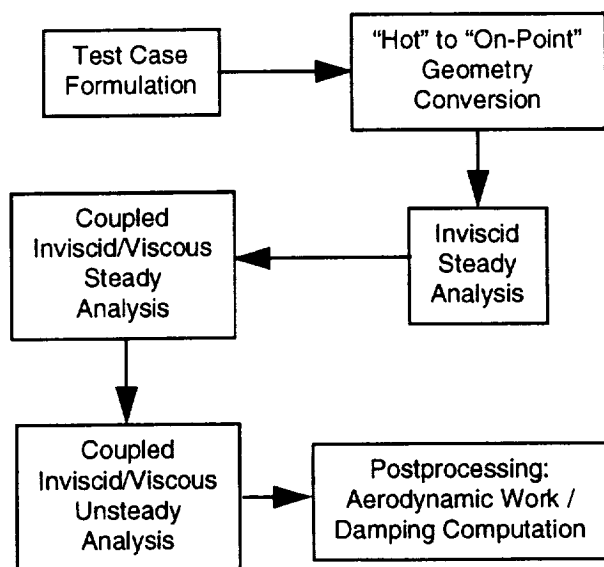


Figure 12. Analysis Methodology Flowchart.



The inviscid computational grid used in these analyses uses a structured H type mesh in the outer region with 20 nodes across the blade passage and 120 points in the flow direction. The viscous equations are solved on an O-grid with 19 nodes normal to the airfoil. A global view of the UNSFLO computational grid is shown in Figure 13 with a detailed view provided to show better resolution of the O-grid. It should be noted that all grid motion is confined to the O-grid and the H-grid remains stationary for the unsteady calculations.

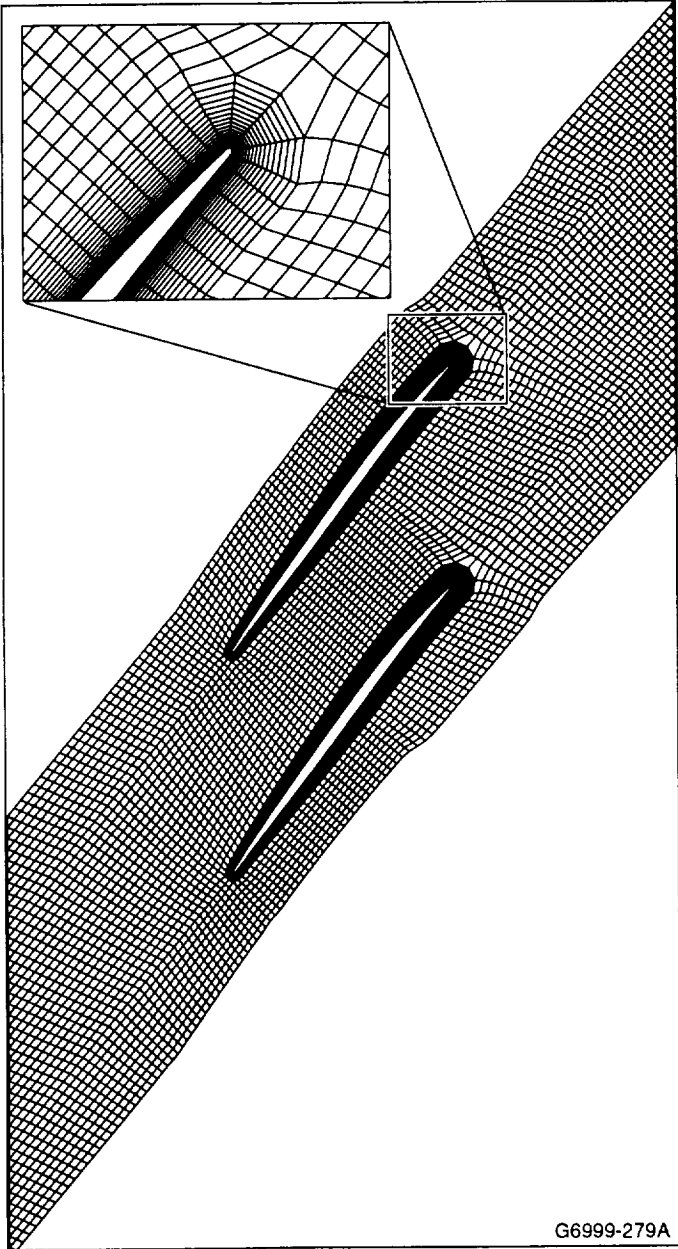


Figure 13. UNSFLO Computational Grid.

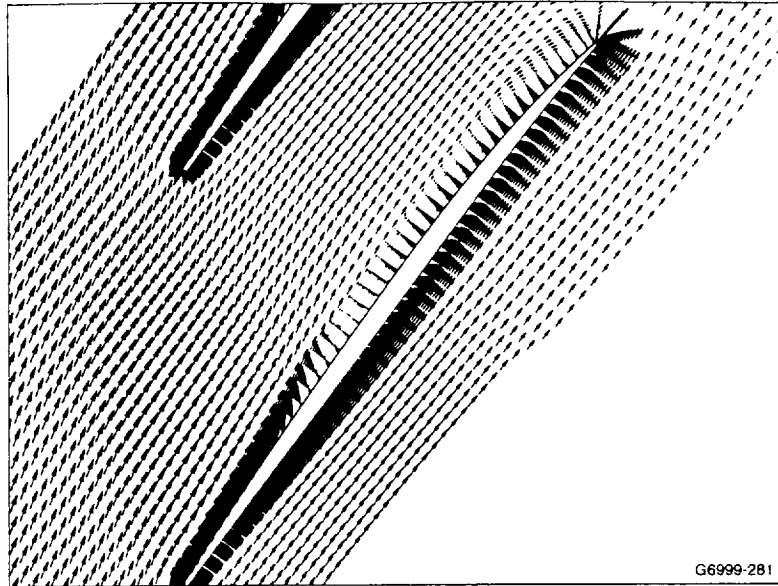
#### **4.2.3.2 Inviscid/Coupled Viscous Solution Results**

Each UNSFLO analysis begins with an inviscid, steady state, solution of the Euler equations of fluid motion. It is not necessary to obtain complete convergence of the inviscid equations to begin the coupled solution. Typically, the authors ran each inviscid solution for 5000 iterations until a reasonably converged solution was obtained.

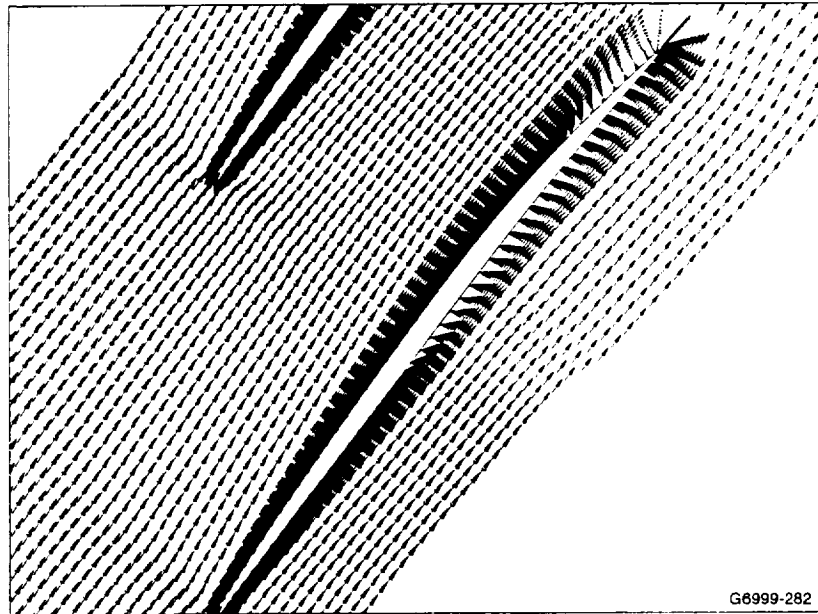
After an inviscid solution is available, the results are interpolated onto the inviscid/viscous grid and the steady coupled solution is initiated. The convergence criteria was chosen so the residual was less than 0.00001 throughout the computational grid. Typically, 50,000 iterations were required to attain convergence of the coupled solution.

Flow vectors from the steady coupled solution are presented in Figure 14(a) for the case F1. Note the flow separation that occurs on the suction side of the airfoil. This situation was not unexpected due to the high incidence angle for this case. The separated flow region is smaller for case NF2. Figure 14(b), as would be expected since the incidence is much lower at the design point.

Comparisons of surface pressure distributions have been completed between UNSFLO and the 3-D viscous steady analysis code DAWES<sup>6</sup>. The UNSFLO results reasonably match the DAWES results as can be seen from Figures 15(a) and 16(a) for cases F1 and NF2 respectively. In addition, UNSFLO steady pressure contours are shown in Figures 15(b) and 16(b) for reference. It should be noted that the DAWES solutions were completed with design point geometry so an exact match with the UNSFLO solution should not be expected.

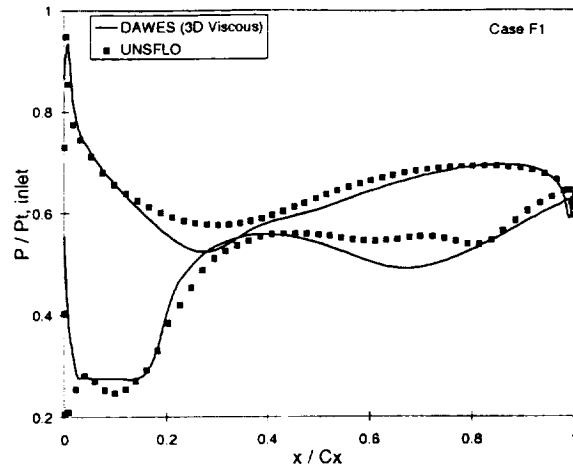


a) Case F1

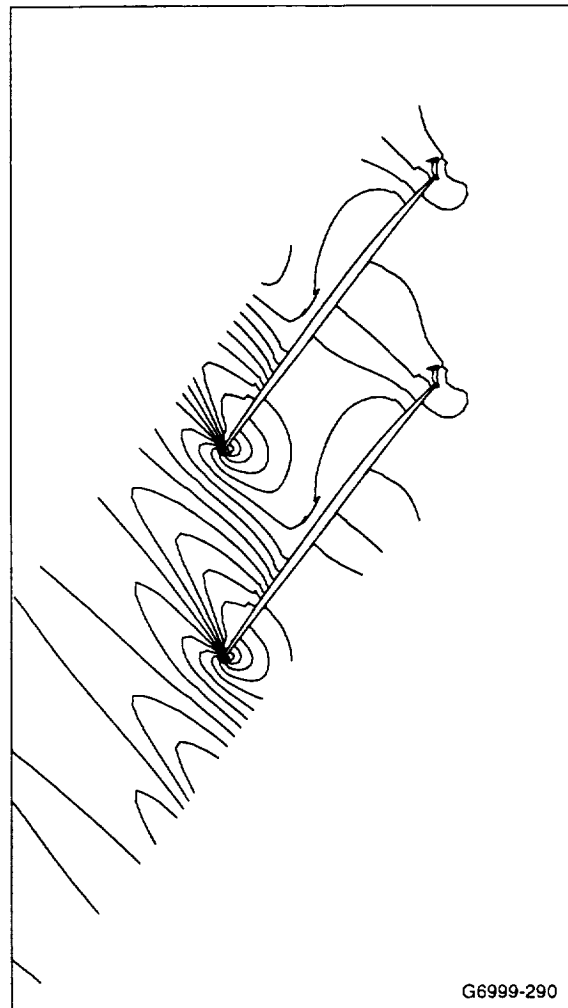


b) Case NF2

**Figure 14. UNSFLO Steady Flow Vectors for Typical Test Cases.**

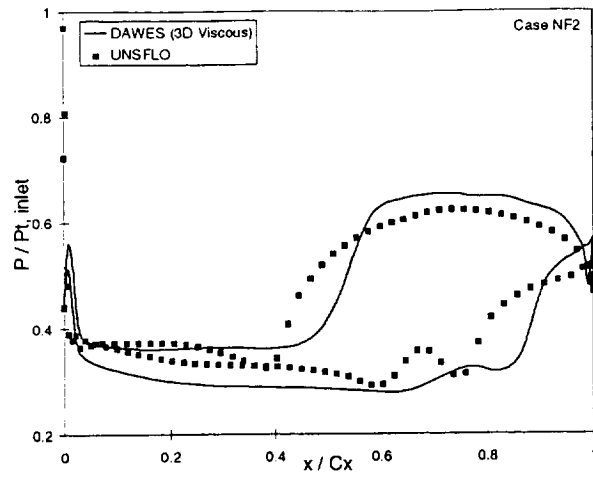


a) Steady Surface Pressures

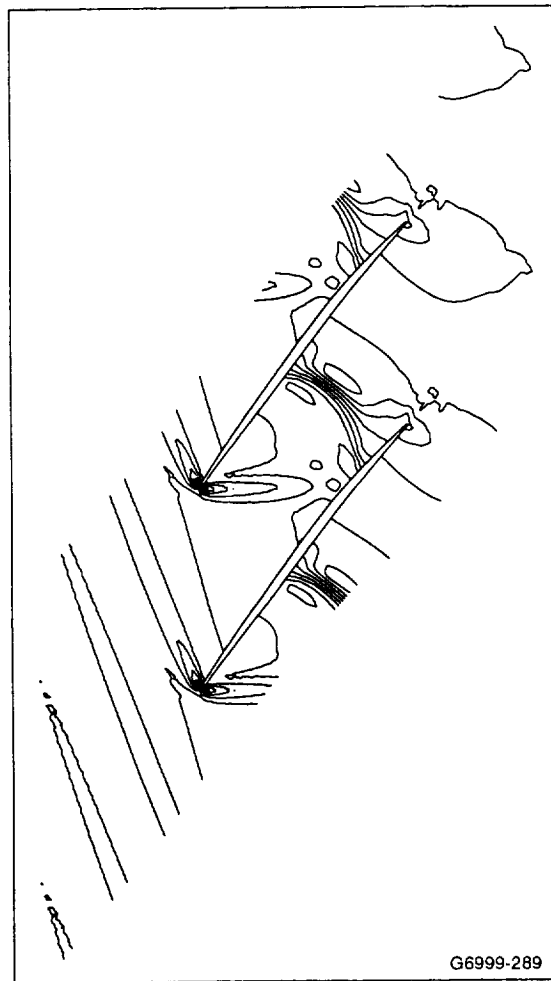


b) Surface Pressure Contours

Figure 15. UNSFLO Steady Results for Case F1.



a) Steady Surface Pressures



b) Surface Pressure Contours

Figure 16. UNSFLO Steady Results for Case NF2.

### 4.2.3.3 Unsteady Flow Comparisons

The unsteady flow solution is determined by oscillating the airfoil in harmonic motion and solving the coupled unsteady aerodynamic equations. As previously mentioned, UNSFLO allows for three vibrational displacements in the x, y, and  $\alpha$  directions. The solution was typically allowed to run for 5 oscillation periods and convergence was verified by a difference between residuals for each period being less than 0.001. Typically, this occurred within the first 3 periods.

The UNSFLO unsteady analyses were completed for two Inter-Blade Phase Angles (IBPA). The first situation (IBPA =  $0^\circ$ ) corresponds to a condition where all airfoils on the rotor vibrate in phase. Additionally, UNSFLO analyses were completed for IBPA =  $32.7^\circ$  corresponding to the actual conditions observed during testing for cases F1 - F6 as determined from strain gage phasing analyses.

A plot of the minimum, average, and maximum, unsteady surface pressures loadings for cases F1 and NF2 can be seen in Figure 17(a) and 18(a) for IBPA =  $0^\circ$ . The variation in surface pressure between minimum and maximum is negligible and the data lines are coincident for both test cases.

A completely different situation is shown for IBPA =  $32.7^\circ$  in Figures 17(b) and 18(b). For case F1, there is a significant variation between the loadings when the airfoil oscillates. This trend does not repeat for case NF2, and the IBPA =  $32.7^\circ$  results are essentially identical to those for IBPA =  $0^\circ$ , as shown in Figure 18(b).

As will be discussed in the following section, it was found that flutter was predicted only for case F1 at IBPA =  $32.7^\circ$  of the four conditions shown in Figures 17 and 18. This situation indicates that the large variations in loading seen in Figure 17(b) are important for aeroelastic stability.

Finally, typical unsteady pressure contour plots are presented in Figures 19 and 20 for IBPA =  $0^\circ$  and  $32.7^\circ$  respectively. Note in symmetry in Figure 19 where the unsteady pressures which are 1/2 period apart have equal but opposite signs. This result should be expected for the IBPA =  $0^\circ$  case where the airfoils vibrate in phase with each other. When IBPA =  $32.7^\circ$  the situation is quite different as seen from Figure 20. In this case, there is no clear symmetry (none should be expected) and further there are streaks evident between blades and also at the interface between the O and H grids. These issues are an area of concern for AE as they indicate that the code may not be fully converged. Further effort will be expended in this area in the future to develop a better understanding of the UNSFLO unsteady flow solutions.

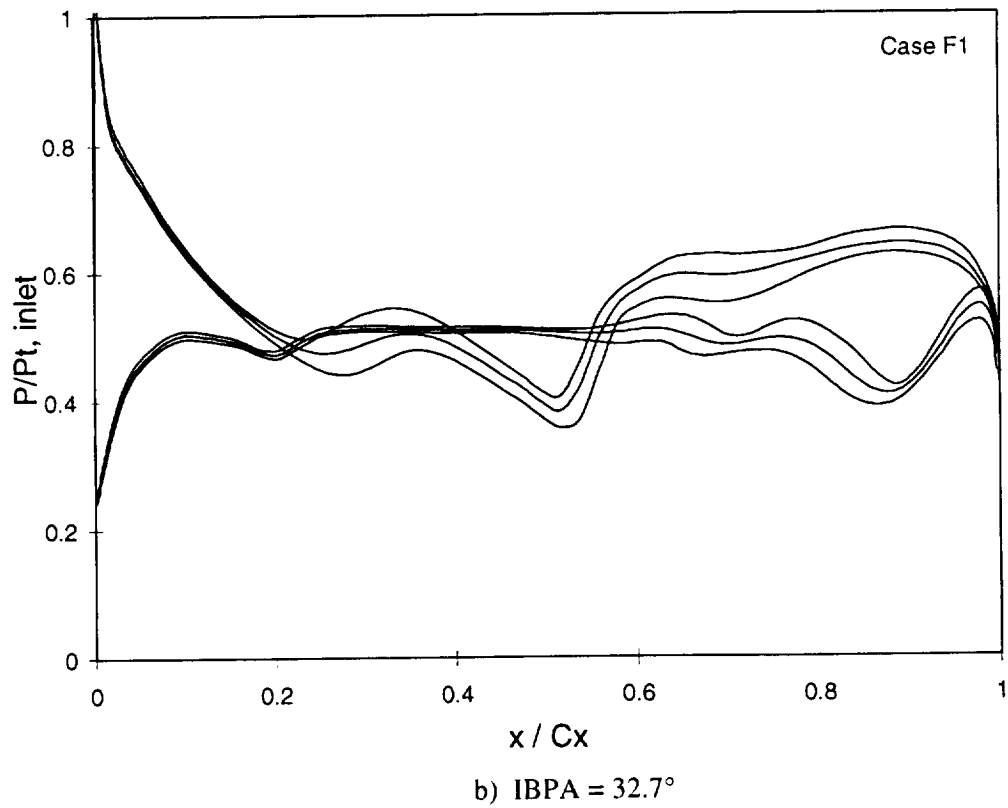
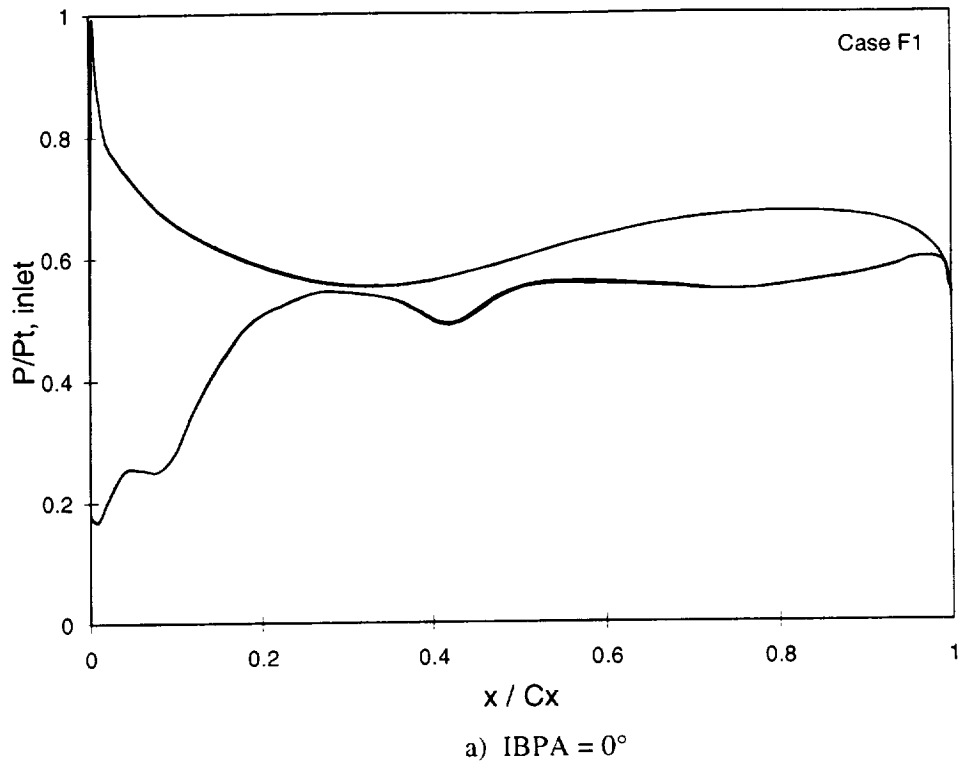
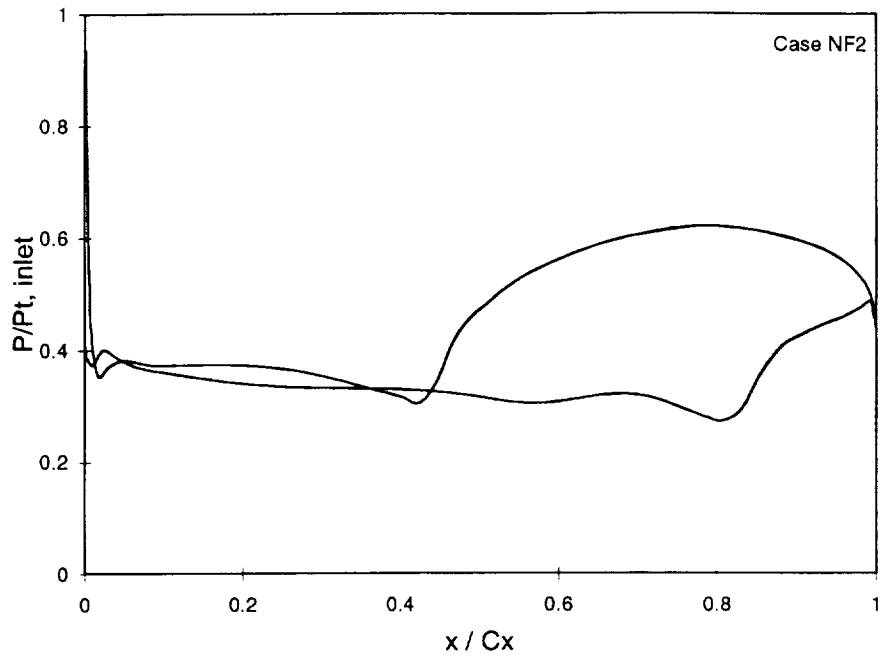
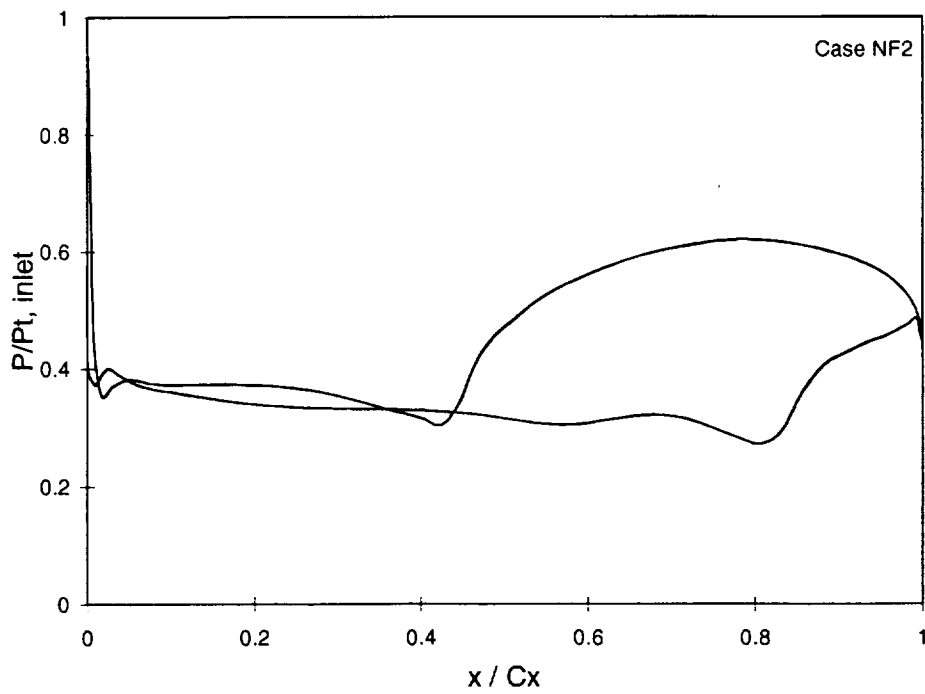


Figure 17. UNSFLO Unsteady Surface Pressures (Max, Min, Average) for Case F1.



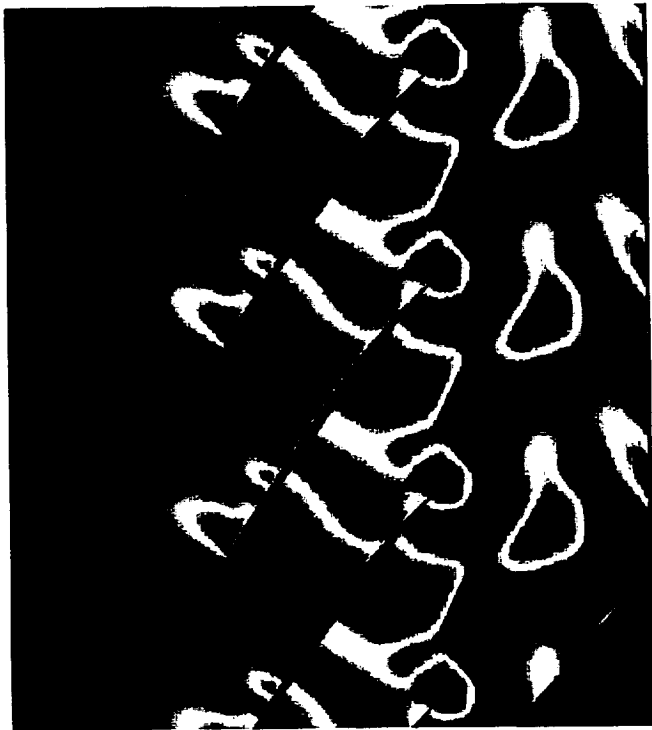
c) IBPA =  $0^\circ$



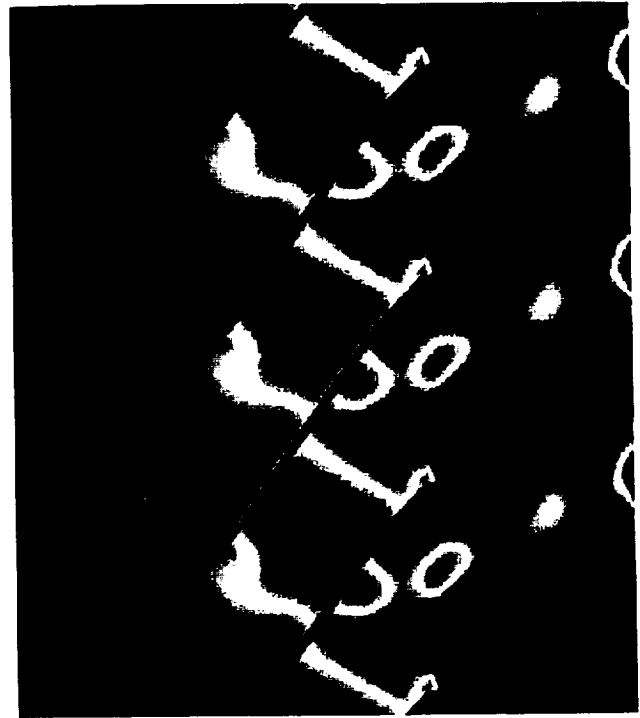
d) IBPA =  $32.7^\circ$

Figure 18. UNSFLO Unsteady Surface Pressures (Max, Min, Average) for Case NF2.

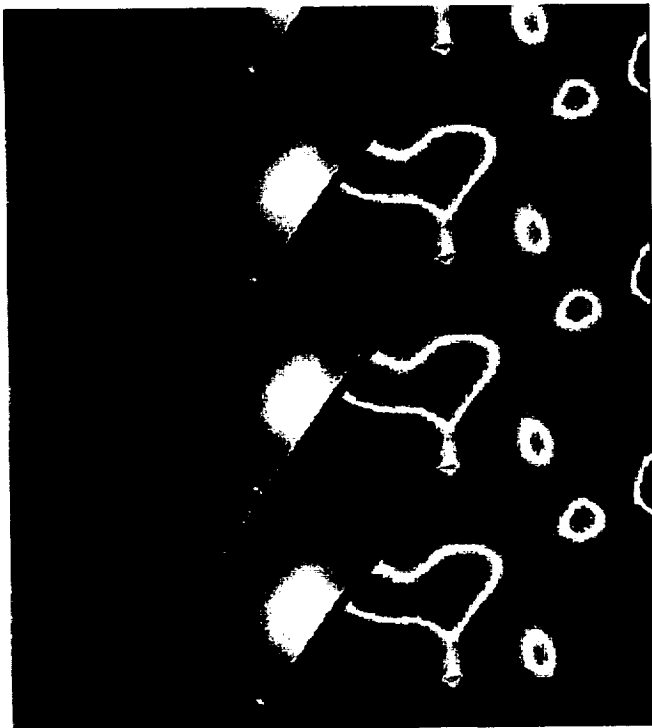




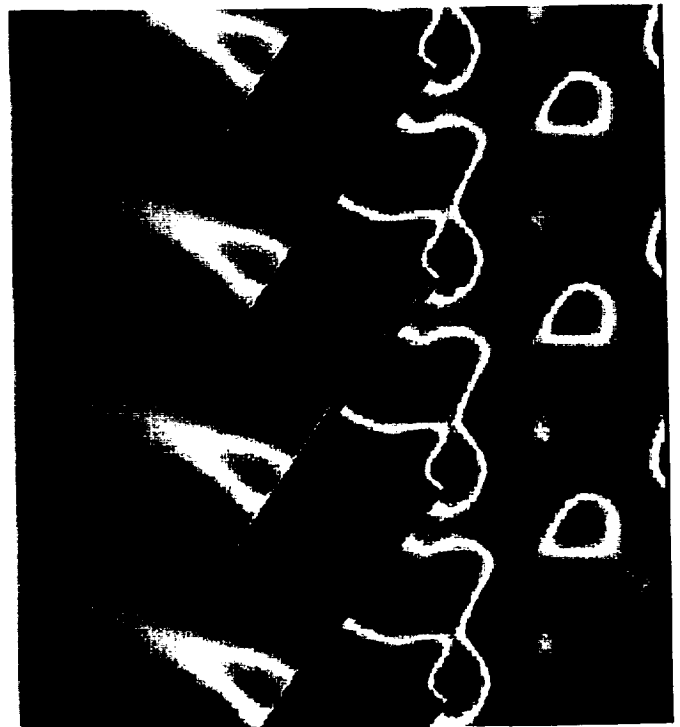
Time t = 0



Time t = 0.25 Cycle

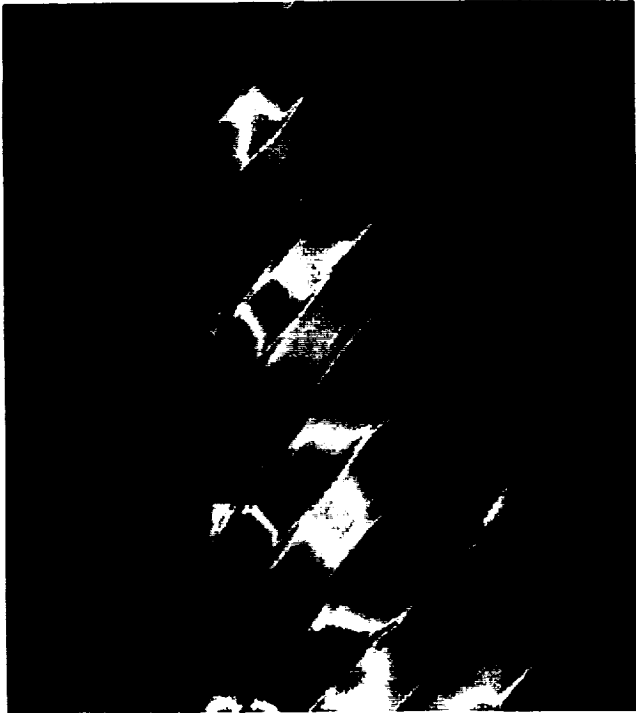


Time t = 0.50 Cycle



Time t = 0.75 Cycle

Figure 19. UNSFLO Unsteady Pressure Contours for Various Times In the Blade Vibrational Cycle (IBPA=0°).



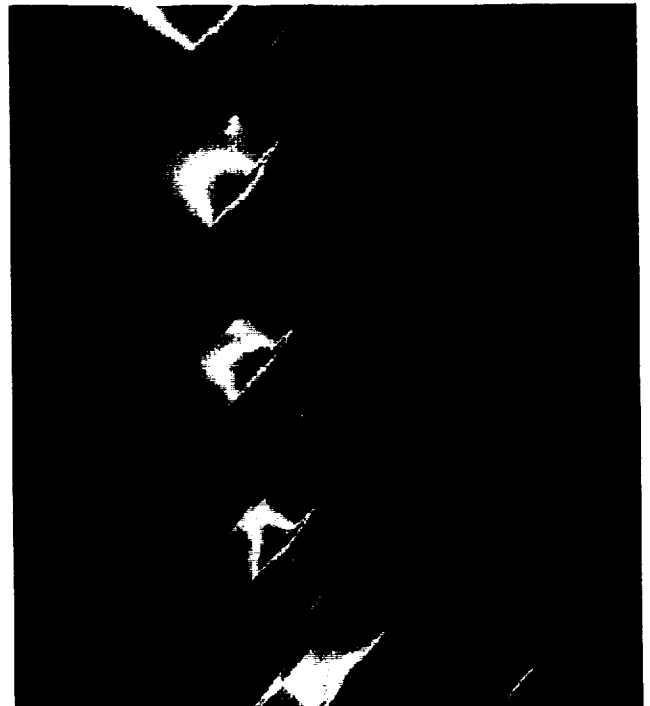
Time  $t = 0$



Time  $t = 0.25$  Cycle



Time  $t = 0.50$  Cycle



Time  $t = 0.75$  Cycle

**Figure 20. UNSFLO Unsteady Pressure Contours for Various Times In the Blade Vibrational Cycle (IBPA=32.7°).**

#### 4.2.3.4 Aerodynamic Damping Computation

Based on the stated objectives of this task, the most important result from the unsteady solution is the postprocessing computation of aerodynamic damping. The first step in this process is to compute the aerodynamic work per vibrational cycle from the equation:

$$W_{\text{per cycle}} = |h_x| |f_x| \sin \varphi_{f_x h_x} + |h_y| |f_y| \sin \varphi_{f_y h_y} + |\alpha| |m_\alpha| \sin \varphi_{m_\alpha \alpha} \quad (1)$$

where  $|h_x|$ ,  $|h_y|$  represent the magnitudes of the mode shape displacements in the translational directions x and y, and  $|\alpha|$  corresponds to the rotational displacement of the blade cross section. The terms  $|f_x|$  and  $|f_y|$  represent the x and y forces and  $|m_\alpha|$  represents the twisting moment on the airfoil. Finally, the term  $\varphi_{re}$  represents the angle in which the response (r) leads the excitation (e).<sup>7</sup>

The aerodynamic damping,  $\Theta$ , was estimated by normalizing the vibrational work per cycle with the leading edge displacement of the airfoil, i.e.

$$\Theta = \frac{W_{\text{per cycle}}}{\pi \delta_{le}} \quad (2)$$

where  $\delta_{le}$  is the magnitude of the leading edge mode shape deflection.

Results from this postprocessing effort are shown in Table 1 for the two values of IBPA previously discussed. It is noted that for each test case, F1 - F6, the UNSFLO predictions indicate negative damping for  $IBPA = 32.7^\circ$ . These predictions match the experimental observations from the rig testing.

The damping prediction is also negative for case NF1 at  $IBPA = 32.7^\circ$  where flutter did not occur on the test rig. However, the magnitude of the damping is small enough that it may not overcome the material structural damping indicating that the design is marginally stable and flutter may not occur. Finally, it should be noted that the damping is predicted to be slightly positive for case NF2. This result matches the experimental observations as flutter was not observed for this test case.

**TABLE 1. UNSFLO AERODYNAMIC DAMPING COMPUTATION FOR AE FAN FLUTTER CASES.**

Test Case	Aerodynamic Damping (%)	
	IBPA = 0°	IBPA = 32.7°
F1	-0.010%	-0.194%
F2	-0.029%	-0.046%
F3	0.014%	-0.041%
F4	0.002%	-0.011%
F5	-0.011%	-0.123%
F6	-0.004%	-0.065%
NF1	-0.001%	-0.004%
NF2	0.000%	0.001%

It should be further noted from Table 1 that the aerodynamic damping decreases for each flutter test case F1 - F6 as IBPA changes from 0° to 32.7°. To quantify this trend, the variation of aerodynamic damping with IBPA was computed for case F2. These results, shown in Figure 21, indicate that the lowest damping was found near IBPA = 32.7°. This situation again matches the experimentally observed results in which the flutter IBPA was measured at 32.7° and provides further validation of the UNSFLO computational tool.

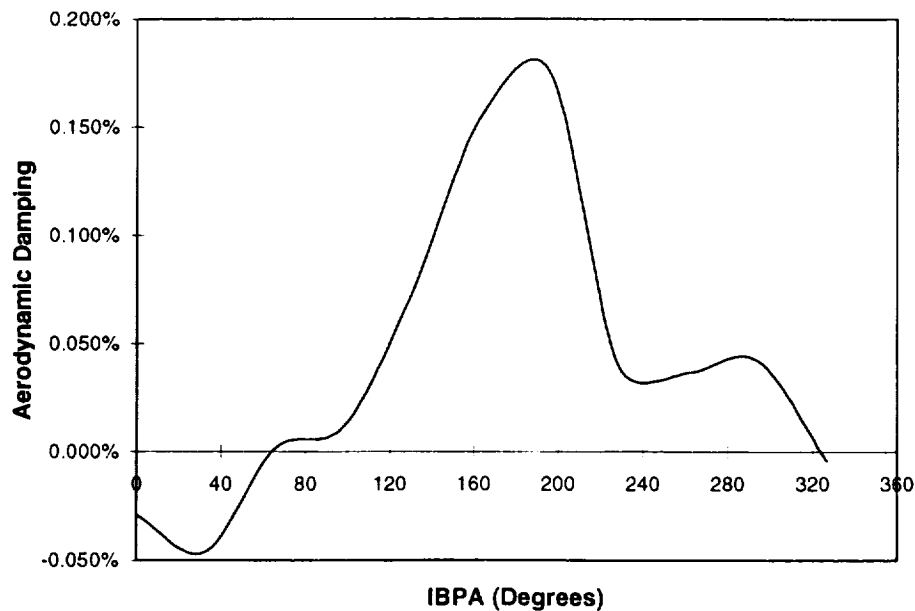


**Figure 21. UNSFLO Variation of Damping with IBPA for Case F2.**

#### **4.2.4 Synchronous Vibrations**

AE completed synchronous vibration analyses for each of the test cases S1 - S6. Unfortunately, there is minimal description on how to perform these computations in the UNSFLO manual. Further, some minor code modifications were required to get the incoming distortion wave to travel in the proper direction. In addition, the results from these analyses (unsteady pressures) are not provided in a form compatible with structural finite element packages. Finally, UNSFLO does not allow blade motion during synchronous vibration analyses so the effect of blade vibration on the unsteady pressure predictions is not determined.

These limitations make the results obtained from the synchronous evaluations of limited value toward the ultimate goal of predicting the vibratory stress amplitude on the fan blisk rotor blades. Typical total pressure contours are shown in Figure 22 for time increments of 0.125 vibrational cycle. The distortion wake is seen entering the blade row in Figure 22(a) and progresses through the passage in Figure 22 (b)-(f).

The AE intent was to have the distortion behave as a square wave with a 2/revolution pattern which would correspond to an entire pressure wave (high pressure and low pressure) over 11 blade passages for the 22 bladed blisk rotor. This situation is observed in Figure 22(c) which shows the high (red) pressure covering approximately 5.5 blades and the low (blue) pressure just entering the blade row.

AE recognizes that significantly more effort is required to interpret and use the unsteady pressure data obtained from these analyses to predict the vibratory response of rotor blades in synchronous vibrations. Further, we do not fully understand the wake generation capability in the UNSFLO code. Developing solutions to these issues will be the focus of AE efforts on future programs.

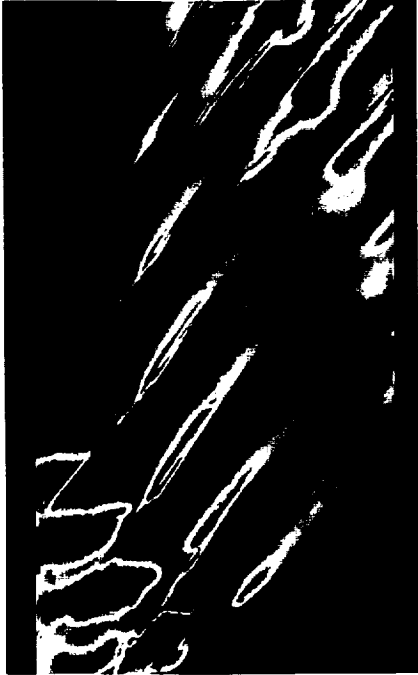
#### **4.2.5 AE Suggestions for Further Development of the UNSFLO Code**

During the course of this effort AE obtained substantial experience operating the UNSFLO code. Several areas for improvement and further study have been suggested and are summarized as follows:

- Utilize the UNSFLO adaptive gridding feature in which a coarse grid is used for the initial solutions and steadily refined in the critical areas.
- Determine the cause of the unsteady pressure anomalies shown in Figure 20 for the  $IBPA = 32.7^\circ$  analyses.
- Validate the phase-lag boundary conditions for several cases by running analyses using multiple blade passages.
- Incorporate the effects of streamtube height into the UNSFLO analyses.

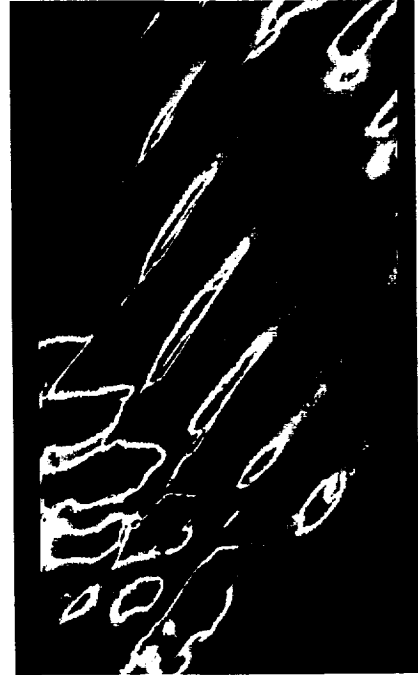
- Develop a post-processor to transfer the synchronous vibration unsteady pressures into a format useful to a structural finite element analysis tool.
- Develop improved distortion wake capabilities for synchronous vibrations.
- Integrate the UNSFLO work per cycle computations into the post-processor rather than performing these computations off-line.
- Determine why the UNSFLO work/cycle computations do not show linear behavior when normalized by (amplitude)<sup>2</sup>.
- Add a feature to incorporate blade motion into synchronous vibration analyses.

These studies/changes will greatly improve the capabilities of the UNSFLO computational tool.



G7017-1

a) Time = 0.000 Cycle



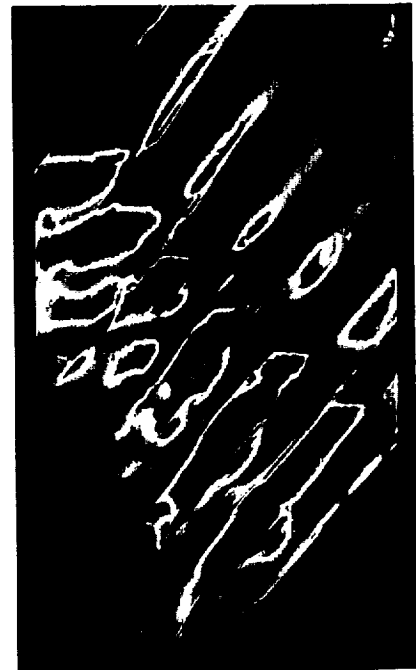
G7017-2

b) Time = 0.125 Cycle



G7017-3

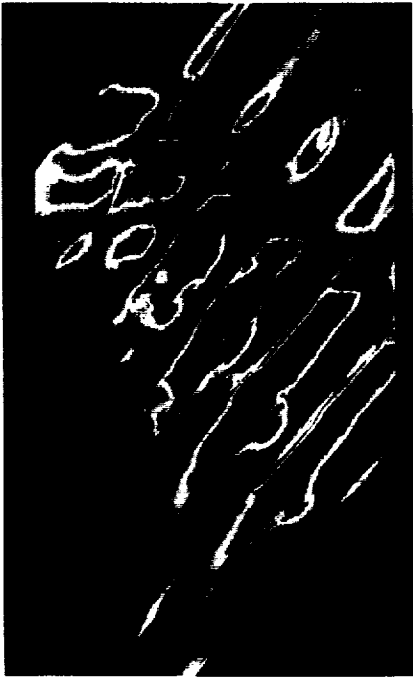
c) Time = 0.250 Cycle



G7017-4

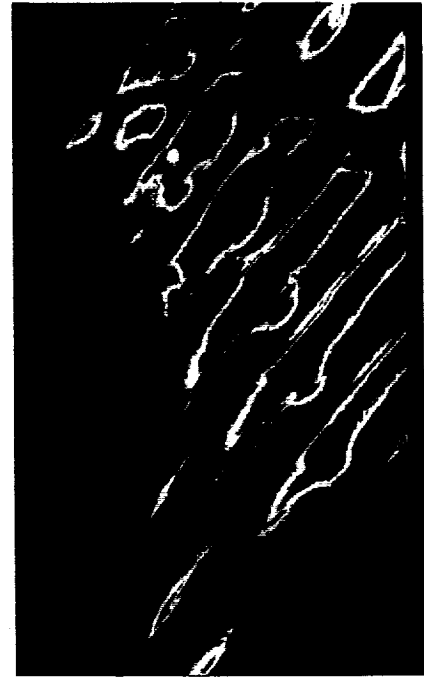
d) Time = 0.375 Cycle

**Figure 22. UNSFLO Synchronous Unsteady Pressure Contours for Synchronous Vibration Case S3.**



G7017-5

e) Time = 0.500 Cycle



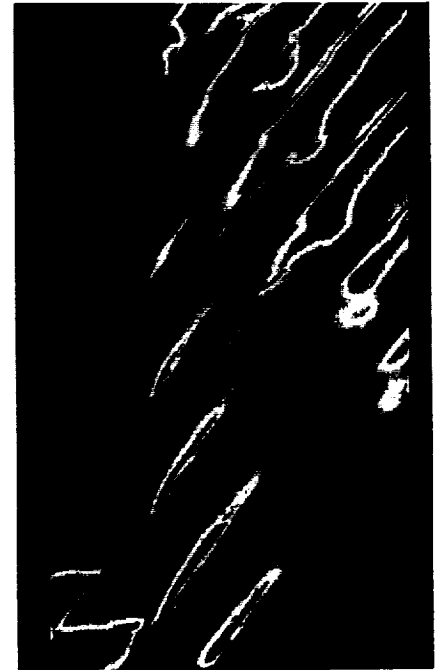
G7017-6

f) Time = 0.625 Cycle



G7017-7

g) Time = 0.750 Cycle



G7017-8

h) Time = 0.875 Cycle

Figure 22. UNSFLO Synchronous Unsteady Pressure Contours for Synchronous Vibration Case S3 (Contd).



### 4.3 Freps Evaluation

#### 4.3.1 General

AE expended a substantial effort on the FREPS code but was unable to evaluate any of the aeroelastic test cases due to operability issues with the steady solver SFLOW. The primary issue is that the initial SFLOW solver released to AE was designed for subsonic flow (designed for Space Shuttle Turbopumps) and all AE fan blisk test cases have transonic flow conditions. A preliminary version of the SFLOW code that was designed for transonic flow was released to AE for evaluation but this code also had difficulty running the blisk test cases. To their credit, it should be noted that this code had not been fully checked out by the NASA researchers prior to release to AE for evaluation.

AE remains fully committed to introducing the FREPS code into our aeroelastic design process as we have a clear need for a fast running preliminary design tool. The execution times discussed in both the UNSFLO and TURBO-AE sections clearly demonstrate the need for this type of tool in a design situation. NASA has recently informed AE about the development of a team to resolve the FREPS efforts and AE is fully supportive of this activity.

#### 4.3.2 Code Description

The FREPS system integrates a structural dynamics analysis with steady and unsteady aerodynamic analyses to perform an aeroelastic analysis. Each analysis (structural, steady, and unsteady aerodynamic) is completed separately and input into the FREPS integration package. The major components are:

- Structural Analysis integration with **MSC/NASTRAN**<sup>8</sup>
- Steady Aerodynamic Solver (**SFLOW**)<sup>9</sup>
- Unsteady Aerodynamic Solver (**LINFLO**)<sup>10</sup>
- Integration Package (**FREPS**)<sup>11</sup>

The order of execution is first to complete the NASTRAN structural and SFLOW steady aerodynamic analyses separately. Next, FREPS is executed and automatically runs the LINFLO routine as required for the aeroelastic analysis at hand.

### 4.3.3 Results



All FREPS test cases (F1 - F6, S1 - S6, OD1, and RD1) have been attempted at four radial spans (25 percent, 50 percent, 75 percent, and 95 percent). These cases were attempted using SFLOW version 1.7 which is designed (but not yet fully tested by NASA researchers) for transonic flow conditions.

Results from this effort are summarized in Table 2 indicating that convergence of the SFLOW code remains a difficulty at the span locations higher than 25 percent. Further, convergence has only been obtained for the SFLOW global solution (solved on a H-grid shown in Figure 23) while AE has not been able to obtain any converged solutions for the local solution (solved on a combined C and H grid). Unfortunately, without having SFLOW results it is not possible to run either the LINFLO or the FREPS programs so the overall code evaluation goals were not completed.

AE has retained all of the SFLOW, LINFLO, and FREPS input decks for all test cases. This will allow quick evaluation of the codes when improved versions of SFLOW are available. These cases will be provided (if requested) to NASA to be used during the code modification process.

**TABLE 2. FREPS COMPLETION STATUS.**

Test Case	SFLOW				LINFLO				FREPS
	25% SPAN	50% SPAN	75% SPAN	95% SPAN	25% SPAN	50% SPAN	75% SPAN	95% SPAN	
F1	Attempted	Completed G	Attempted	Attempted	Attempted	Attempted	Attempted	Attempted	Attempted
F2	Attempted	Completed G	Attempted	Attempted	Attempted	Attempted	Attempted	Attempted	Attempted
F3	Attempted	Attempted	Attempted	Attempted	Attempted	Attempted	Attempted	Attempted	Attempted
F4	Attempted	Completed G	Attempted	Attempted	Attempted	Attempted	Attempted	Attempted	Attempted
F5	Completed G	Completed G	Attempted	Attempted	Attempted	Attempted	Attempted	Attempted	Attempted
F6	Completed G	Completed G	Attempted	Attempted	Attempted	Attempted	Attempted	Attempted	Attempted
S1	Completed G	Completed G	Attempted	Attempted	Attempted	Attempted	Attempted	Attempted	Attempted
S2	Completed G	Completed G	Attempted	Attempted	Attempted	Attempted	Attempted	Attempted	Attempted
S3	Attempted	Attempted	Attempted	Attempted	Attempted	Attempted	Attempted	Attempted	Attempted
S4	Attempted	Attempted	Attempted	Attempted	Attempted	Attempted	Attempted	Attempted	Attempted
S5	Completed G	Attempted	Attempted	Completed G	Attempted	Attempted	Attempted	Attempted	Attempted
S6	Completed G	Attempted	Completed G	Completed G	Attempted	Attempted	Attempted	Attempted	Attempted
OD1	Completed G	Attempted	Attempted	Attempted	Attempted	Attempted	Attempted	Attempted	Attempted
RD1	Completed G	Attempted	Attempted	Attempted	Attempted	Attempted	Attempted	Attempted	Attempted

Attempted   
 Completed   
 G = Global Solution Converged  
 L = Local Solution Converged

#### **4.3.4 Further Explanation of SFLOW Problem Areas**

The difficulties in converging the SFLOW code can be seen from Figure 24 which shows the SFLOW computed Mach numbers at 75 percent span for a typical test case. This situation is also shown in Figure 25 (vector length indicates the flow velocity) where the flow velocity spikes significantly overspeed and the code will not converge. This difficulty occurred even when the inlet Mach number was lowered to a value substantially less than the appropriate level for the test case.

AE ran our 3-D Euler solver (DENTON) on one of the test cases and these results are presented in Figure 26. Note that the leading edge Mach number does indeed increase but not nearly to the level of the SFLOW solver. AE, under the NASA AST Task 14 program plus internal funds, looked into bypassing the SFLOW solver and using the DENTON results in the FREPS module. This concept appears feasible and has the advantage of eliminating the need for an additional code to be entered into the AE design system.

During these analyses AE attempted to make grid variations to the H-grid based on the parameters described in the FREPS input manual. The allowable grid changes are the number of points on the blade, number of points from inlet boundary to leading edge, number of points from trailing edge to exit boundary, number of points between blade, and the grid spacing. Varying these parameters did not yield any substantial reduction in the convergence difficulties.

#### **4.3.5 AE Suggestions for SFLOW/FREPS Code Improvements**

AE has several suggestions that we would like to see incorporated into the FREPS module. These items have been presented to NASA personnel at various meetings and telecons and will be repeated here for convenience.

- Update SFLOW to handle transonic flow conditions. In order to facilitate this activity, AE is willing to let the code developers use one of our test cases.
- Incorporate streamtube height corrections into the SFLOW and LINFLO. Our experience with UNSFLO has shown that streamtube height significantly affects results. This effect is very pronounced on a fan.
- Modify FREPS to handle structural finite element results from different packages. Our suggestion here is to use the TURBO-AE structural input file format.
- Improve user manuals for SFLOW and LINFLO. These codes are described in minimal detail in the appendices of the FREPS manual. Unfortunately, FREPS is inoperable without these codes so manuals are very important. Note that we felt FREPS had an excellent user's manual.

- Consider developing an interface package so engine companies can use their own steady flow solvers. This option would be very valuable to AE as we already have a fully calibrated steady design tool (DENTON) and would prefer not to use another code.

These improvements will substantially improve operability of the FREPS code if they are incorporated. As previously mentioned, AE has a strong need for a quick turnaround aeroelastic analysis tool for design analyses. It is anticipated that the updated version of FREPS or its 3-D counterpart (FREED) will be used for this purpose.

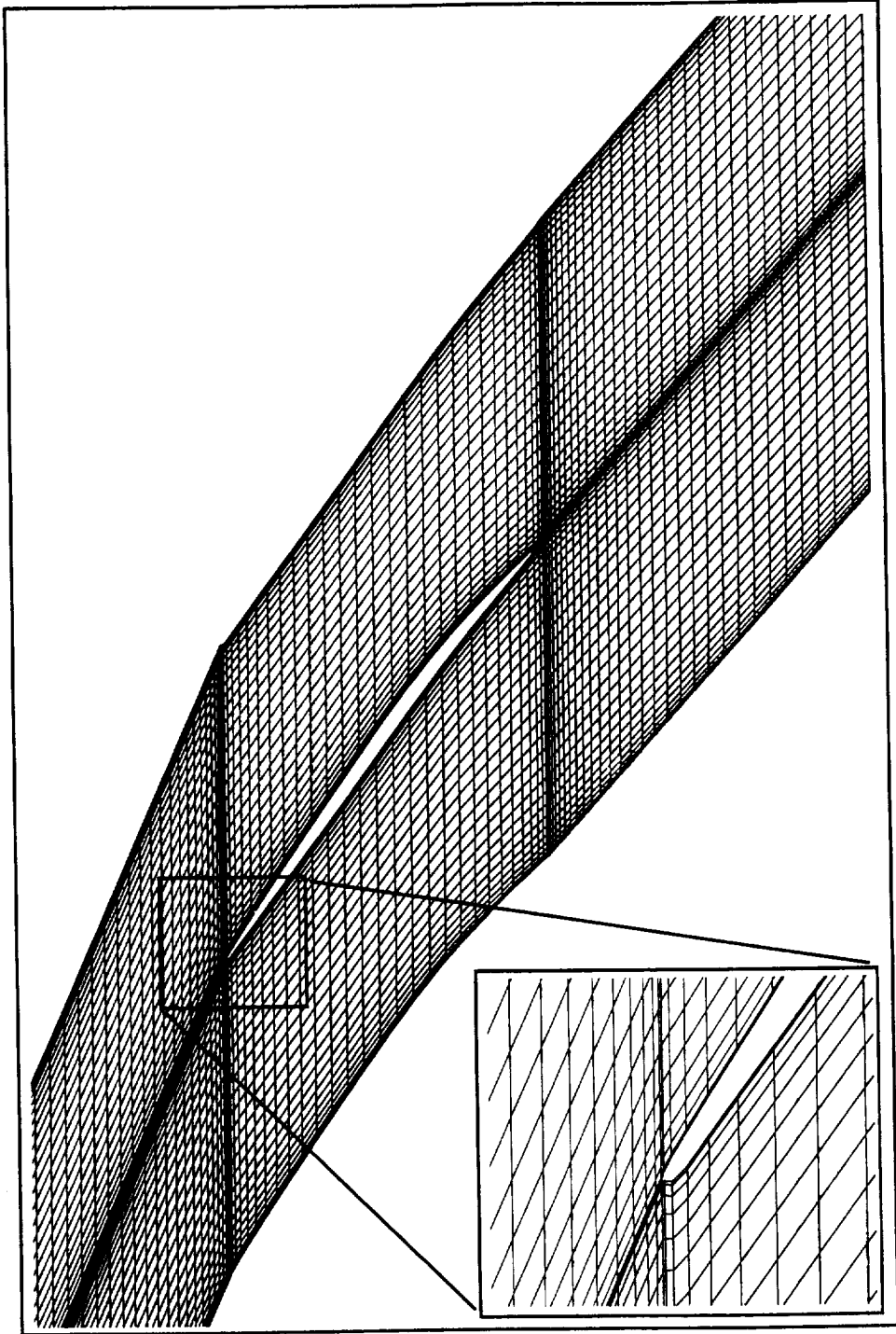


**Figure 23. Typical SFLOW Computational H-Grid.**

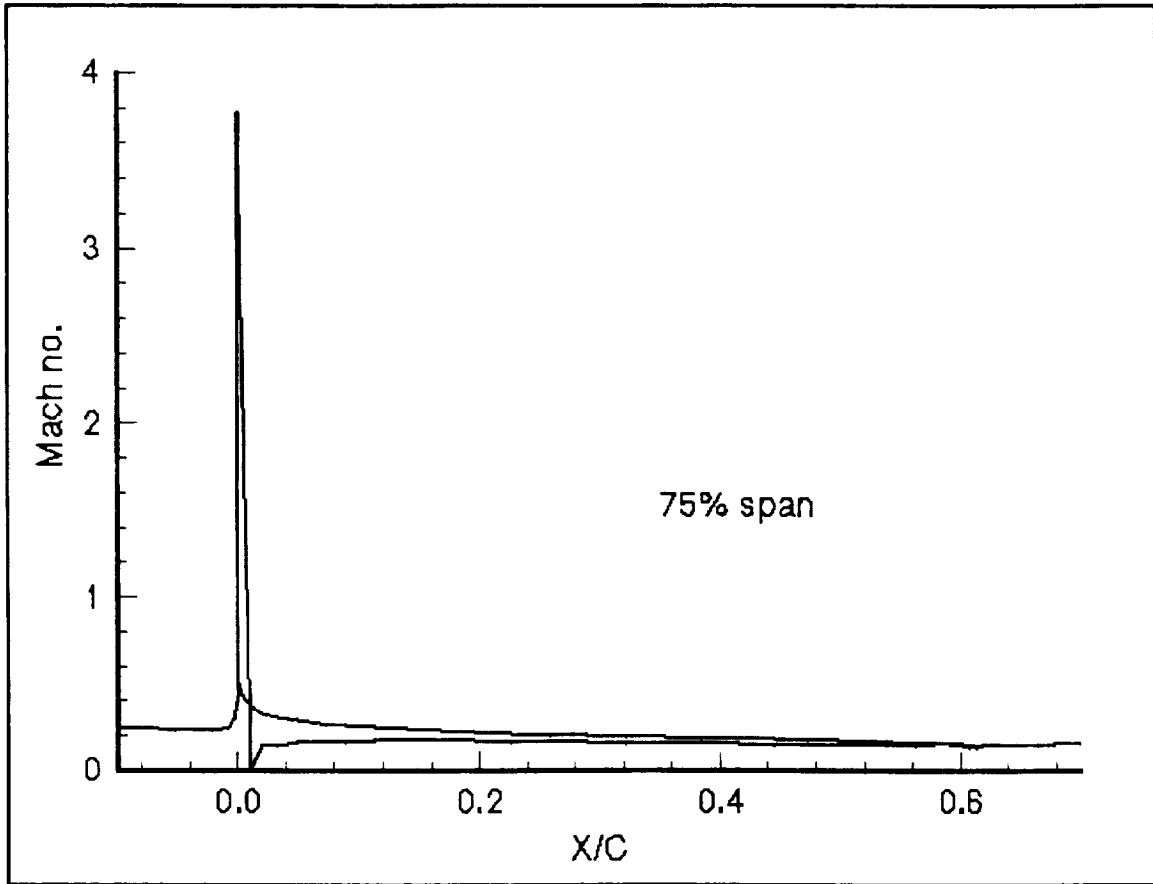


**Figure 24. SFLOW Solution has a Leading Edge Mach Number Overspeed for All Test Cases.**

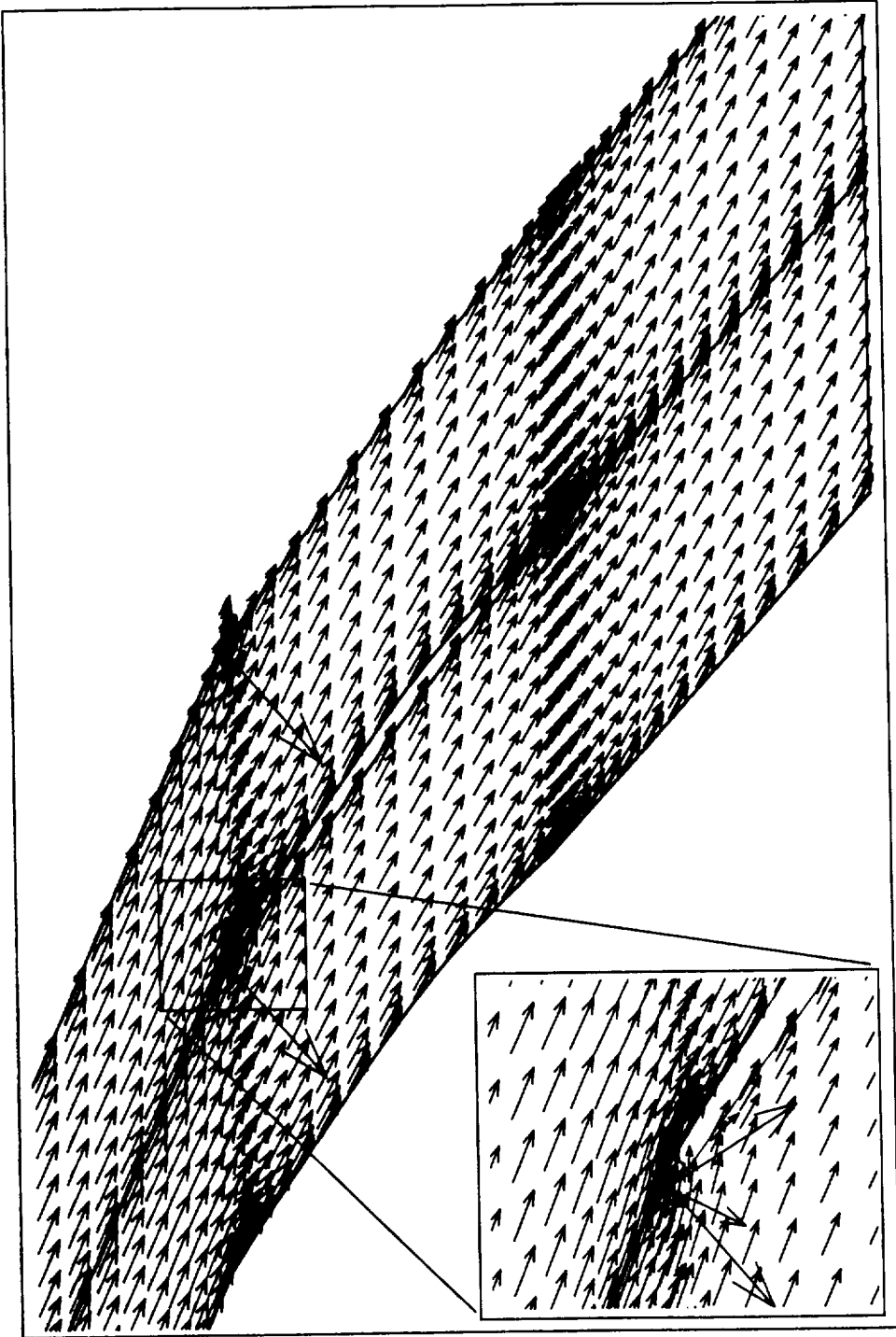
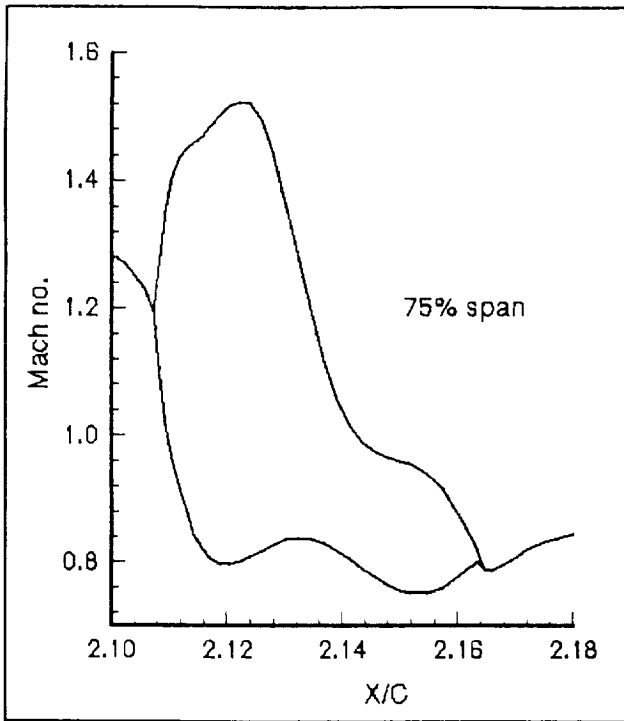
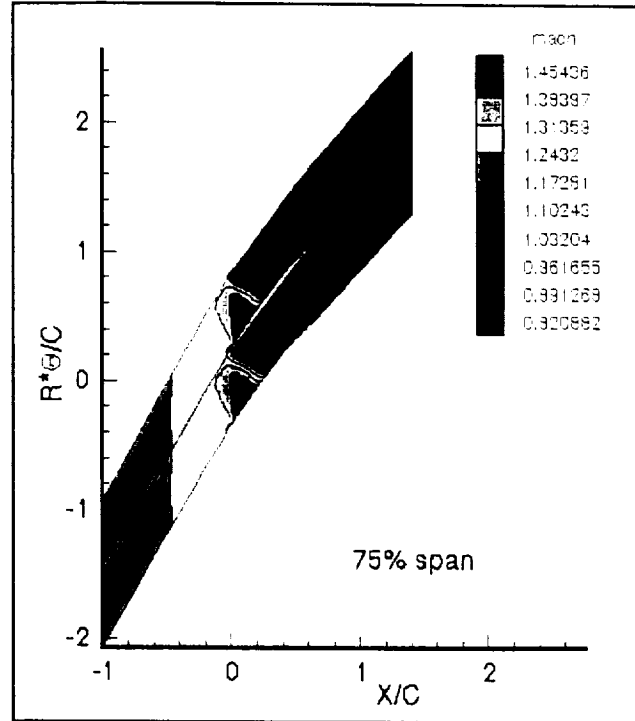


Figure 25. SFLOW Flow Vectors Show Overspeed at Leading Edge.



Surface Mach number



Mach Number Contours

Figure 26. 3-D Euler Code (DENTON) Results for Typical FREPS Case.



## **4.4 Turbo-AE Evaluation**

### **4.4.1 General**

The goal for the TURBO-AE evaluation was to run one of the flutter test cases with the currently available version of the code. AE chose the F2 case (see Figure 10 and Table 1) as the case to analyze for this task. The choice of the F2 case was random and all of the other F, S, and NF cases will be run under the AST Task 6 program.

The TURBO-AE code was made available to AE in the third quarter of 1996. Initially, it was anticipated that NASA would supply computer time on their CRAY machine to run the test cases for the SET Task 8 program. However, scheduling issues arose and it was not possible to use the CRAY for this program. Due to this limitation, AE installed the TURBO-AE code on our HP workstation network. AE is pleased that the events worked out this way as we now have a much better understanding of the code through the many trouble shooting issues that arose in installing it on the HP workstation network.

Please note that the code version supplied to AE for this effort had the original (not non-reflecting) inlet and exit boundary conditions. All results presented in this report are for this version of the code. It should also be noted that the viscous routine in TURBO-AE had a problem during this program and AE was asked by NASA to complete all analyses with viscous calculations turned off.

### **4.4.2 Code Description**

The aeroelastic analysis code TURBO-AE is under development at NASA Lewis Research Center<sup>12</sup>. The starting point for the development was an Euler/Navier-Stokes unsteady aerodynamic code named TURBO which was generated at Mississippi State University<sup>13, 14</sup>. Routines have been developed to interpolate the structural deflections from the finite-element grid to the CFD grid. Grid deformation routines have been developed to calculate a new grid for the deformed blade at each time step. Routines have been developed for the calculation of work and generalized forces. These routines have been verified by running the code for a standard configuration.

The TURBO code was originally developed as an inviscid flow solver for modeling the flow through multistage turbomachinery. It has the capability to handle multiple blade rows with even or uneven blade count, stationary or rotating blade rows and blade rows at an angle of attack. Multiple blade passages are included in the calculation, when required. Additional developments were made to incorporate viscous terms into the model. The code can now be applied to model realistic turbomachinery configurations with flow phenomena such as shocks, vortices, separated flow, secondary flows, and shock and boundary layer interactions.

TURBO is based on a finite volume scheme. Flux vector splitting is used to evaluate the flux Jacobians on the left hand side of the governing equations and Roe's flux difference splitting is used to form a higher-order TVD (Total Variation Diminishing) scheme to evaluate the fluxes on the right hand side. Newton sub-iterations are used at each time step to maintain higher accuracy. A Baldwin-Lomax algebraic turbulence model is used in the code.

The TURBO-AE code assumes a normal mode representation of the structural dynamics of the blade. Thus, the dynamic characteristics of each blade are assumed to be represented in terms of in-vacuum modes, with the associated natural frequency and generalized mass for each mode. Typically, a finite-element analysis code such as ANSYS is used to calculate the modal data mentioned. A work-per-cycle approach is used to determine aeroelastic (flutter) stability. Using this approach, the motion of the blade is prescribed to be a harmonic vibration in a specified in-vacuum normal mode with a specified frequency. The vibration frequency is typically the natural frequency for the mode of interest, but some other frequency can also be used. The aerodynamic forces acting on the vibrating blade and the work done by these forces on the vibrating blade during a cycle of vibration are calculated. If work is being done on the blade by the aerodynamic forces, the blade is dynamically unstable, since it will result in extraction of energy from the flow, leading to an increase in amplitude of oscillation of the blade. Note that coupled mode flutter cannot be modeled with this approach.

A limitation of TURBO-AE is that it currently requires calculations over multiple blade passages for blade motions with non-zero interblade phase angle. For a typical propulsion component, fan, compressor, or turbine, this can lead to very large computational requirements in CPU time and memory. Hence, in the future, the code will be extended to allow the analysis of arbitrary interblade phase angles using a single blade passage. This can be accomplished by using a single blade passage with time (or phase) shifted boundary conditions. Also, it is necessary that the TURBO-AE code be exercised to evaluate its ability to analyze and predict flutter for conditions in which viscous effects are significant. This is also planned for the future.

#### **4.4.3 NASA E<sup>3</sup> Fan Test Case**

After installing TURBO-AE we performed a checkout using the NASA supplied E<sup>3</sup> test case for both the steady and unsteady runs. These results (steady and unsteady) matched those obtained from the NASA CRAY C-90 results with excellent accuracy as seen from Figure 27 which presents the aerodynamic work performed on the airfoil for 8 vibrational cycles. This experience gave us confidence in the installation and we moved on to running the F2 test case.

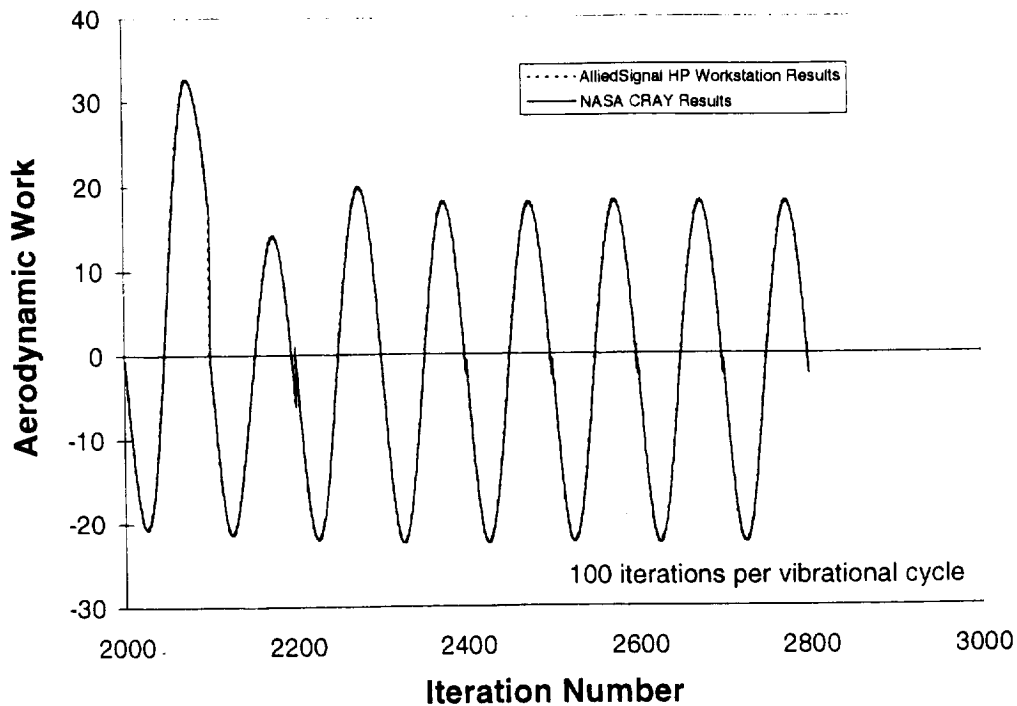


Figure 27. Comparison of NASA and AlliedSignal Unsteady Results for the E<sup>3</sup> Fan.

#### 4.4.4 Flutter Vibrations on F2 Test Case

Several minor and a few significant code modifications were required to get the TURBO-AE code to execute using the AE F2 test case. Many of these issues were related to problem size as the CFD grid for the F2 case had substantially more grid points than the NASA supplied E<sup>3</sup> test case. Each issue was resolved and AE has completed numerous analyses successfully.

The computational grid chosen for the analyses is shown in Figure 28. This grid (90x35x25) is coarser than AE typically uses (131x71x25) with our DAWES 3-D viscous analyses. AE chose not to run an extended grid (upstream and downstream) of the blade row to account for the absence of non-reflecting boundary conditions. The implications of this choice will be evaluated when the non-reflecting boundary condition version of the code becomes available during the AST Task 6 program.

#### 4.4.5 Steady Results

AE completed numerous analyses in order to get the steady TURBO-AE results. Most of these runs had run-time errors for various reasons including improper grid choices, dimensioning errors, script errors, etc. When these issues were finally resolved, the TURBO-AE code ran flawlessly on the F2 steady case.

The first step in evaluating the TURBO-AE steady results was to compare the loading diagrams to those obtained from our calibrated DAWES 3-D viscous design code. These results are shown in Figures 29 and 30 for mid and 95 percent spans respectively. The agreement between TURBO-AE and DAWES is very impressive, especially when considering that TURBO-AE had a coarser grid and the viscous computations were deferred. Discussions with AE CFD experts reached the conclusion that this agreement was as good as can be expected when comparing two computational tools.

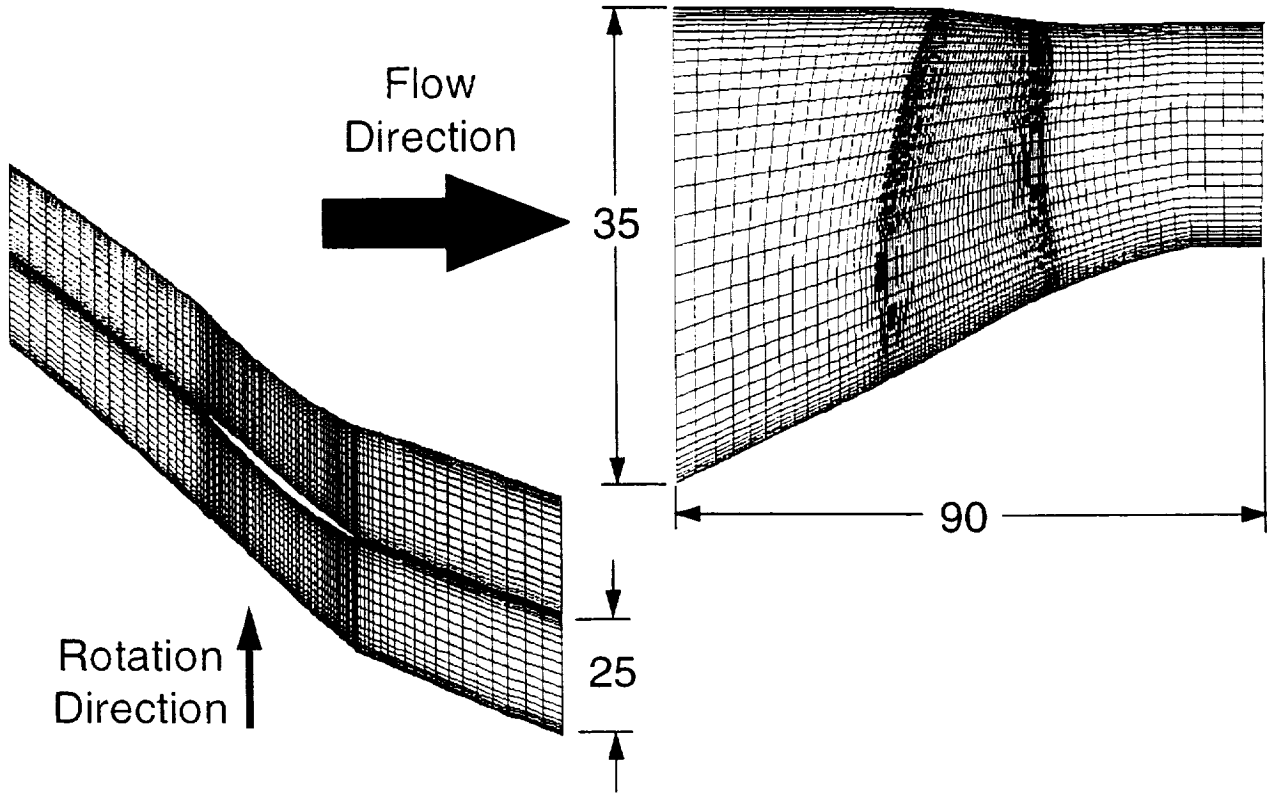


**Figure 28. Computational Grid For TURBO-AE Analyses.**

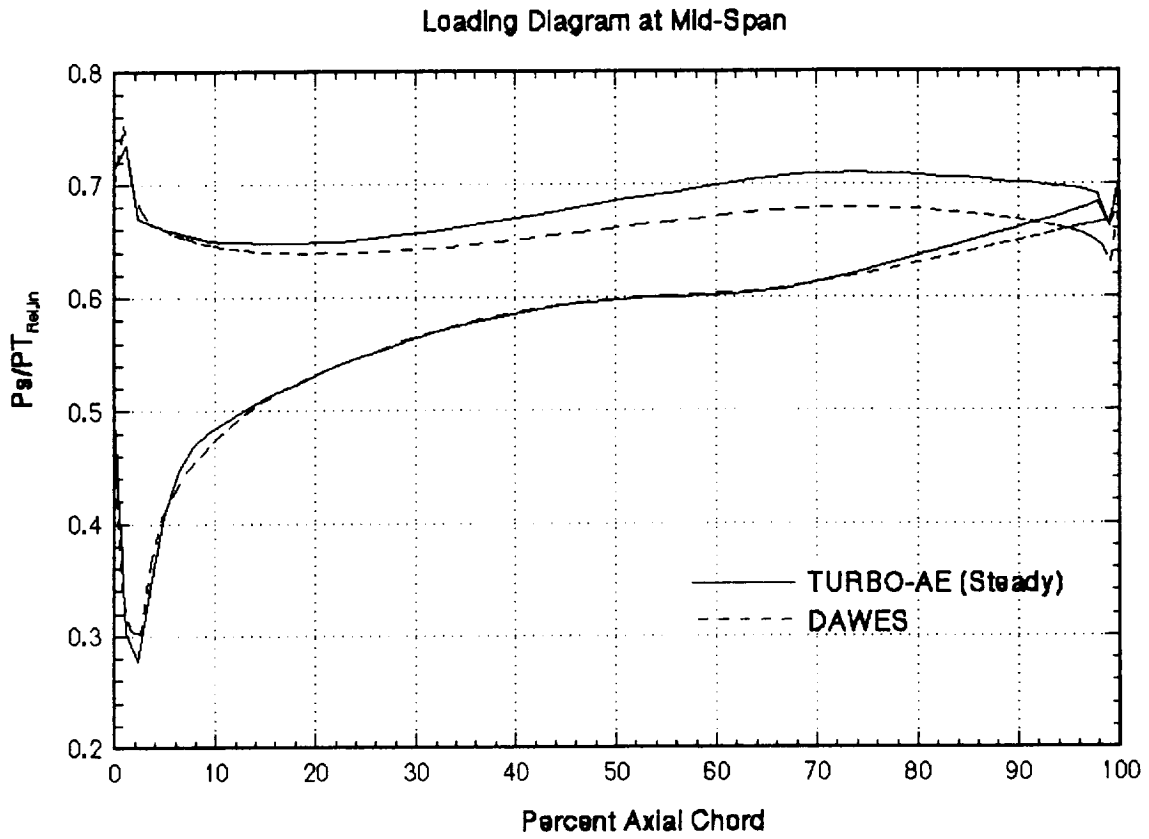


**Figure 29. Steady Flow TURBO-AE/DAWES Comparison for Case F2 at Mid-Span.**

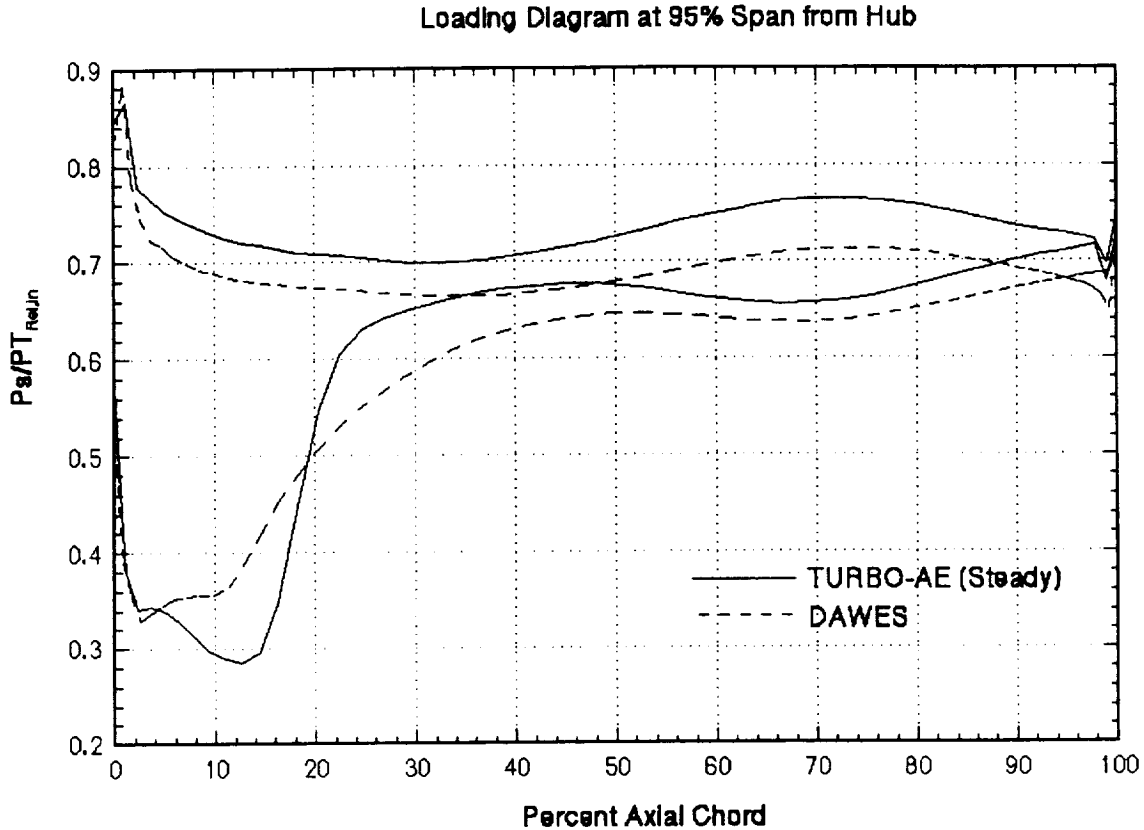


**Figure 30. Steady Flow TURBO-AE/DAWES Comparison for Case F2 at 95 Percent Span.**

#### **4.4.6 Unsteady Results**

As with the steady analyses, the unsteady runs required many attempts to get the execution scripts and TURBO-AE code to run properly. After these issues were resolved, numerous analyses were completed.

The initial runs were completed for IBPA = 0° and 180° and varied both the vibration amplitude and the number of iterations per vibratory cycle. Results from this effort are presented in Table 5 and are described in the following paragraphs.

Examining first the IBPA = 0° case, the vibration amplitude was varied from 0.003 to 0.300 in multiples of 10 and the results are presented in the first three rows of Table 5. The aerodynamic work/cycle result showed linear behavior for 0.003 and 0.030 amplitudes which is clearly seen from the normalized work/cycle (work/cycle/(amplitude)<sup>2</sup>) which remained in the 225 range for both amplitudes. The 0.300 amplitude run had an execution error which is not unexpected as this case represents a substantial amount of grid motion. For reference, note that the iterations per vibrational cycle were chosen at 400 for all cases in the first 6 rows of Table 5.

The IBPA = 180° runs produced similar results to the IBPA = 0° analyses as can be seen from rows 4 through 7 in Table 3. The work/cycle indicated that the code was operating in the linear region and the 0.300 vibration amplitude case would not run. One interesting point is that the work/cycle for IBPA = 180° is much higher than the IBPA = 0° analyses. Another important issue is that the work/cycle is nearly equivalent for both passages in the IBPA = 180° analyses. This result is obviously consistent with expectations. As previously mentioned, the number of iterations per period was chosen as 400 for all of these runs.

The next step in the evaluation process was to determine the sensitivity of the work/cycle to the number of iterations per vibratory cycle. This situation was evaluated by completing additional runs at 200 and 800 iterations/period for IBPA = 0° and 180° with the vibration amplitude set at 0.003. These results are presented in rows 6 through 12 of Table 3. The first issue to note is that the 200 iterations per period cases would not execute since the time step was too large. The 400 iterations/period are simply repeats of the previous cases. Finally, the 800 iterations/period cases show inconsistent results for IBPA = 0° in that the work/cycle substantially reduces over the 400 iterations/period case. The IBPA = 180° cases did not show this inconsistency as the normalized work/cycle is nearly constant for both 400 and 800 iterations/period. This issue was discussed with several NASA researchers and the general consensus was that the anomalies were likely caused by the lack of non-reflecting boundary conditions. AE will re-run these cases with the non-reflecting BC version of the code when it becomes available.

The final TURBO-AE case completed for SET Task 8 was to run the IBPA = 32.7° case which corresponds to the condition where flutter was observed on the rotor. This case requires 11 blade passages to be modeled and the ISSD=1 option was used in the code. The analysis required approximately 12 days to complete and the results are given in Table 4 indicating that TURBO-AE is predicting flutter for this condition. The normalized work/cycle is reasonably consistent for all 11 passages. NASA researchers have found a minor coding issue that may further improve the consistency of the work/cycle between passages. These changes have been incorporated and will be evaluated during the AST Task 6 contract. Another interesting point from Table 4 is that the results did not change substantially after the first vibrational cycle. If this result holds true for all cases, the run time can be substantially reduced from 12 to 3 days which is far more reasonable for design type analyses. AE is in the process of obtaining substantially faster computers which will also reduce the analysis time.

Finally, the work per cycle for the 400 iteration/period and 0.003 amplitude is plotted against IBPA in Figure 31. As previously noted, flutter was observed on the rotor for IBPA = 32.7°. The TURBO-AE code predictions indicate that work/cycle is positive for this condition so it can be stated that the code did indeed predict flutter at the observed flutter point. However, the highest work/cycle prediction occurred at IBPA = 180°. It is not clear to AE at the present time if flutter has to occur at the highest work/cycle condition. We will take this issue under consideration during the upcoming AST Task 6 program.

**TABLE 3. TURBO-AE UNSTEADY RESULTS FOR CASE F2 WITH IBPA = 0° AND 180°.**

		Work / Cycle		Work/(Amplitude) <sup>2</sup>	
IBPA	Amplitude	Passage 1	Passage 2	Passage 1	Passage 2
0	0.003	0.0019	-	210.7	-
0	0.030	0.2108	-	234.2	-
0	0.300	*	-	*	-
180	0.003	0.0208	0.0211	2307.8	2345.3
180	0.030	2.0607	2.0625	2289.7	2291.7
180	0.300	*	*	*	*

\* Amplitude too large for code convergence

		Work / Cycle		Work/(Amplitude) <sup>2</sup>	
IBPA	Iterations/ Period	Passage 1	Passage 2	Passage 1	Passage 2
0	200	**	**	**	**
0	400	0.2108	-	234.2	-
0	800	0.1237	-	137.4	-
180	200	**	**	**	**
180	400	2.0607	2.0625	2289.7	2291.7
180	800	2.3734	2.3707	2637.1	2634.1

\*\* Execution error after fourth vibration cycle

**TABLE 4. TURBO-AE UNSTEADY RESULTS FOR CASE F2 WITH IBPA = 32.7°.**

Normalized Work Per Cycle													
Vibr. Cycle	Passage Number											Avg.	Range
	1	2	3	4	5	6	7	8	9	10	11		
1	854	898	900	860	825	828	855	875	859	823	815	854	85
2	795	819	849	852	812	771	769	795	806	797	791	805	83
3	799	813	822	819	799	784	778	777	773	778	791	794	49
4	795	808	812	812	801	793	778	766	759	771	785	789	53



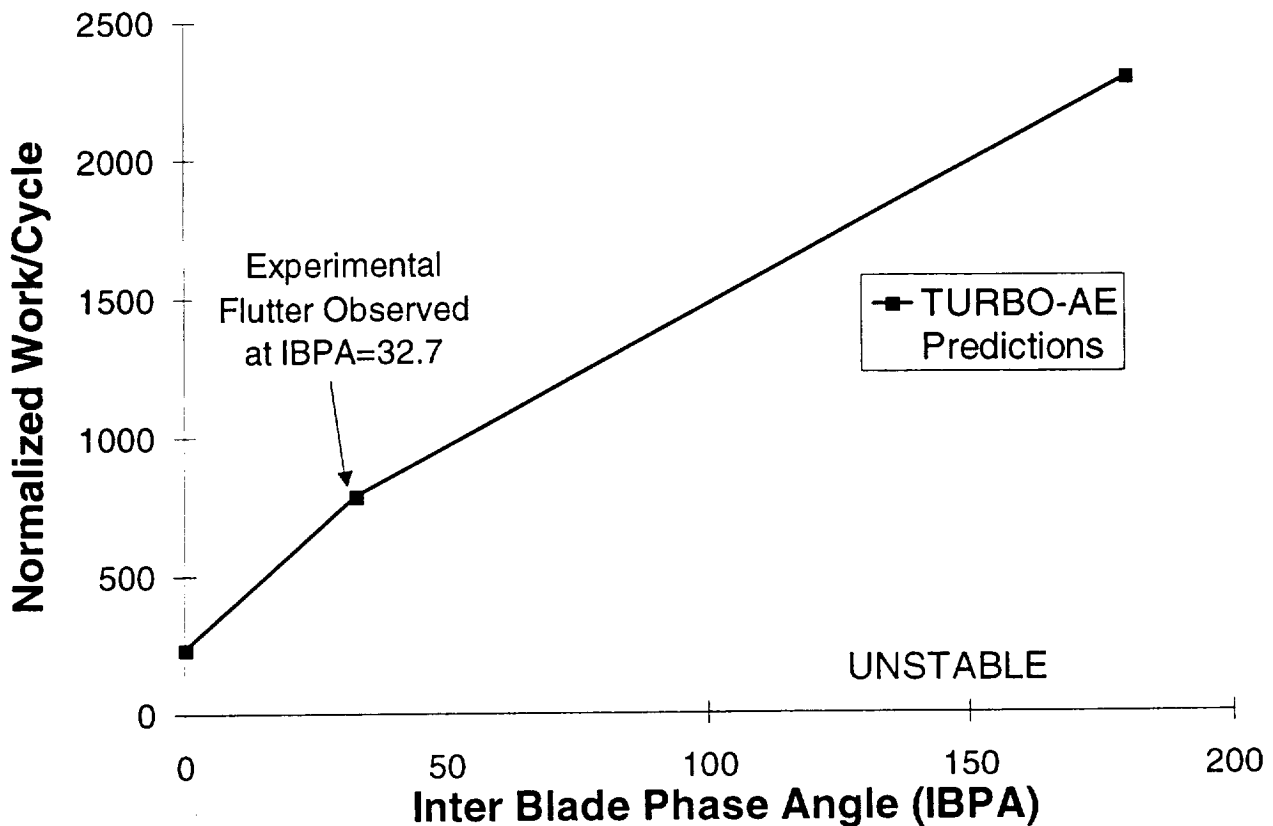


Figure 31. Test Case F2 TURBO-AE Work/Cycle Results for Various Inter Blade Phase Angles.

#### 4.4.7 Go-Forward Plan For Turbo-AE

The AE go-forward plan for TURBO-AE is to continue aggressively running the code on the various flutter conditions for our fan blisk cases. We plan to fully investigate the viscous solver, determine whether our solutions are grid independent, verify the minimum number of iterations per period, and understand the effects of vibration amplitude (especially in the nonlinear range). Further, we have made various design changes that both reduced and also increased the size and intensity of the flutter. We plan to test some of these cases to see the ability of TURBO-AE to synthesize the experimental results.

## 5.0 SUMMARY

During the course of this program (August 1995 through December 1996) AE has made significant progress toward our goal of upgrading our technology to include CFD type aeroelastic analyses. Prior to 1995, all aeroelastic analyses were completed using empirical correlations while we now have capability to complete substantially more detailed analyses.

The UNSFLO flutter analyses were completed for six cases where flutter was observed on the AE fan blisk rotor. UNSFLO did predict negative aerodynamic damping at each of these cases for the 75 percent radial span location analyzed. Further, UNSFLO predicted positive and slightly negative aerodynamic damping for two cases which were flutter free. These results indicate that UNSFLO is a useful tool for the evaluation of flutter on transonic fan rotors.

In addition to flutter, UNSFLO was exercised to evaluate synchronous test cases. While the code was able to complete the required analyses, there is not a link available to transfer the unsteady pressures to a structural finite element code for further analysis. This link, when developed, will enable the user to compute the vibratory strain amplitude for cases involving synchronous vibrations.

The FREPS evaluation was bogged down due to difficulties converging the SFLOW solver which provides a steady flow aerodynamic solution for use with the LINFLO and FREPS modules. Unfortunately, there is no way to complete the FREPS aeroelastic analyses without the SFLOW solution. AE expended substantial effort trying to make SFLOW converge but were unable to achieve that result for any of the test cases attempted. Several suggestions for code improvements were suggested to NASA in this report. It is hoped that NASA will be able to resolve the SFLOW issues as AE has a strong need for a fast turn around aeroelastic analysis tool.

AE was especially pleased with the TURBO-AE results for the single fan flutter case evaluated. In this case, TURBO-AE was able to predict positive aerodynamic work per cycle indicating that flutter would be expected. The steady flow solution matched well with AE's 3-D calibrated DAWES predictions. For unsteady results, three inter blade phase angles were analyzed and the code performed reliably for each case.

NASA AST Task 6 is a follow-on program to the current SET effort which will continue the AE effort to validate advanced aeroelastic computer codes. Under AST Task 6, AE will complete the remaining flutter and synchronous test cases on TURBO-AE along with expanding our efforts to include turbine cases for all three codes.

# REPORT DOCUMENTATION PAGE

*Form Approved*  
OMB No. 0704-0188

Public reporting burden for this collection of information is estimated to average 1 hour per response, including the time for reviewing instructions, searching existing data sources, gathering and maintaining the data needed, and completing and reviewing the collection of information. Send comments regarding this burden estimate or any other aspect of this collection of information, including suggestions for reducing this burden, to Washington Headquarters Services, Directorate for Information Operations and Reports, 1215 Jefferson Davis Highway, Suite 1204, Arlington, VA 22202-4302, and to the Office of Management and Budget, Paperwork Reduction Project (0704-0188), Washington, DC 20503.

<b>1. AGENCY USE ONLY</b> ( <i>Leave blank</i> )	<b>2. REPORT DATE</b> June 1998	<b>3. REPORT TYPE AND DATES COVERED</b> Final Contractor Report	
<b>4. TITLE AND SUBTITLE</b> Small Engine Technology (Set) Task 8 Aeroelastic Prediction Methods Final Report		<b>5. FUNDING NUMBERS</b>  WU-538-06-13-00 NAS3-27483	
<b>6. AUTHOR(S)</b>  Chris D. Eick and Jong-Shang Liu			
<b>7. PERFORMING ORGANIZATION NAME(S) AND ADDRESS(ES)</b> AlliedSignal Engines 111 S. 34th Street P.O. Box 52180 Phoenix, Arizona 85072		<b>8. PERFORMING ORGANIZATION REPORT NUMBER</b>  E-10674 21-9157	
<b>9. SPONSORING/MONITORING AGENCY NAME(S) AND ADDRESS(ES)</b> National Aeronautics and Space Administration Lewis Research Center Cleveland, Ohio 44135-3191		<b>10. SPONSORING/MONITORING AGENCY REPORT NUMBER</b>  NASA CR-1998-202328	
<b>11. SUPPLEMENTARY NOTES</b>  Project Manager, David Janetzke, Structures and Acoustics Division, NASA Lewis Research Center, organization code 5930, (216) 433-6041.			
<b>12a. DISTRIBUTION/AVAILABILITY STATEMENT</b>  Unclassified - Unlimited Subject Category: 07  This publication is available from the NASA Center for AeroSpace Information, (301) 621-0390.		<b>12b. DISTRIBUTION CODE</b>  Distribution: Nonstandard	
<b>13. ABSTRACT</b> ( <i>Maximum 200 words</i> ) AlliedSignal Engines, in cooperation with NASA LeRC, completed an evaluation of recently developed aeroelastic computer codes using test cases from the AlliedSignal Engines fan blisk database. Test data for this task includes strain gage, light probe, performance, and steady-state pressure information obtained for conditions where synchronous or flutter vibratory conditions were found to occur. Aeroelastic codes evaluated include the quasi 3-D UNSFLO (developed at MIT and modified to include blade motion by AlliedSignal), the 2-D FREPS (developed by NASA LeRC), and the 3-D TURBO-AE (under development at NASA LeRC). Six test cases each where flutter and synchronous vibrations were found to occur were used for evaluation of UNSFLO and FREPS. In addition, one of the flutter cases was evaluated using TURBO-AE. The UNSFLO flutter evaluations were completed for 75 percent radial span and provided good agreement with the experimental test data. Synchronous evaluations were completed for UNSFLO but further enhancement needs to be added to the code before the unsteady pressures can be used to predict forced response vibratory stresses. The FREPS evaluations were hindered as the steady flow solver (SFLOW) was unable to converge to a solution for the transonic flow conditions in the fan blisk. This situation resulted in all FREPS test cases being attempted but no results were obtained during the present program. Currently, AlliedSignal is evaluating integrating FREPS with our existing steady flow solvers to bypass the SFLOW difficulties. The TURBO-AE steady flow solution provided an excellent match with the AlliedSignal Engines calibrated DAWES 3-D viscous solver. Finally, the TURBO-AE unsteady analyses also matched experimental observations by predicting flutter for the single test case evaluated.			
<b>14. SUBJECT TERMS</b>  Aeroelasticity; Computational fluid dynamics; Fan blade disk (blisk)		<b>15. NUMBER OF PAGES</b> 62	
		<b>16. PRICE CODE</b> A04	
<b>17. SECURITY CLASSIFICATION OF REPORT</b> Unclassified	<b>18. SECURITY CLASSIFICATION OF THIS PAGE</b> Unclassified	<b>19. SECURITY CLASSIFICATION OF ABSTRACT</b> Unclassified	<b>20. LIMITATION OF ABSTRACT</b>

## 6.0 REFERENCES

- <sup>1</sup> ANSYS Users Manual, Volume IV, "Theory", 1st Revision, September 30th, 1994, refer to: [ansysinfo@ansys.com](mailto:ansysinfo@ansys.com).
- <sup>2</sup> Giles, M. B., 1991, "UNSFLO: A Numerical Method for the Calculation of Unsteady Flow in Turbomachinery," MIT Gas Turbine Laboratory Report.
- <sup>3</sup> Giles, M. B. and Haimes, R. 1993, "Validation of a Numerical Method for Unsteady Flow Calculations," ASME Journal of Turbomachinery, Vol. 115, pp. 110-117.
- <sup>4</sup> Abhari, R. S., Guenette, G. R., Epstein, A. H., Giles, M. B. 1992. "Comparison of Time-Resolved Turbine Rotor Heat Transfer Measurements and Numerical Calculations," ASME Journal of Turbomachinery, Vol. 115, pp. 762-770.
- <sup>5</sup> R.S. Abhari and M. Giles, 1995, "A Navier Stokes Analysis of Airfoils in Oscillating Transonic Cascades for the Prediction of Aerodynamic Damping", ASME Paper 95 GT 182.
- <sup>6</sup> W. N. Dawes, 1986 "A Numerical analysis of the Three-Dimensional Viscous Flow in a Transonic compressor Rotor and Comparison With Experiment." ASME Paper 86-GT-16.
- <sup>7</sup> J. M. Verdon, AGARD No. 298. "Aeroelasticity in Axial-Flow Turbomachines. Volume 1. Unsteady Turbomachinery Aerodynamics: Chapter 2: Linearized Unsteady Aerodynamic Theory," pp. 2-18.
- <sup>8</sup> McCormick, C. W., ed.; MSC/NASTRAN Users Manual, Vol. I and II, MacNeal-Schwendler, 1983.
- <sup>9</sup> Hoyniak, D. and Verdon, J.M., "Development of a Steady Potential Solver for Use with Linearized, Unsteady Aerodynamic Analyses," NASA TM 105288, September, 1991.
- <sup>10</sup> Verdon, J.M., and Caspar, J.R., "Development of a Linearized Unsteady Aerodynamic Analysis for Finite-Deflection Subsonic Cascades," AIAA Journal, Vol. 20, pp. 1259-1267.
- <sup>11</sup> Morel, M.R., and Murthy, D. V., "Turbomachinery Forced Response Prediction System: (FREPS) Users Manual", NASA CR 194465, March, 1994.
- <sup>12</sup> Bakhle, M. A. et al., 1996, "Development of an Aeroelastic Code Based on an Euler/Navier-Stokes Aerodynamic Solver" , ASME Paper 96-GT-311.
- <sup>13</sup> Janus, J. M., 1989, "Advanced 3-D CFD Algorithm for Turbomachinery", Ph.D. Dissertation, Mississippi State University, Mississippi.
- <sup>14</sup> Chen, J. P., 1991, "Unsteady Three-Dimensional Thin-Layer Navier-Stokes Solutions for Turbomachinery in Transonic Flow", Ph.D. Dissertation, Mississippi State University, Mississippi.